

## APPENDIX 3.AN: DYNA3D ANALYSES OF HI-TRAC SIDE DROPS AND IMPACT BY A LARGE TORNADO MISSILE

### 3.AN.1 INTRODUCTION

This appendix considers the HI-TRAC transfer cask response to two different transient accident events; namely, (1) a side drop onto a horizontal target surface from a specified height, and (2), a side impact from a large tornado missile. The analyses are performed as part of Load Cases 02.b and 04 (see Table 3.1.5), respectively. All dynamic analyses are performed using the dynamic finite element code DYNA3D (also known as LS-DYNA3D). This code has been approved for use in this class of problems by the NRC in previous submittals (HI-STAR 100), and has been benchmarked in an approved topical report. DYNA3D has also been used in Appendix 3.A to examine handling accidents involving a loaded MPC contained in the HI-STORM 100 overpack.

The first analysis in this appendix simulates a handling accident that results in a drop of the loaded HI-TRAC (Load Case 02.b in Table 3.1.5). The side drop accident considers the HI-TRAC in a horizontal orientation with its lowest point at a specified elevation above the target. Two initial orientations of the transfer cask are considered to bound all potential side drop accidents. For this case, the only loads considered to lead to high stresses are the inertia loads from the deceleration. It is noted that an alternate analysis of the handling accident has also been performed using a rigid body model of the HI-TRAC System to provide a confirmatory analysis.

The second analysis in this appendix simulates a strike on the HI-TRAC water jacket by a large tornado missile (Load Case 04 in Table 3.1.5). The consequences of a large tornado missile strike are examined by assuming that the vehicle strike is simulated by a specified impact force-time impulse applied over a fixed area of the water jacket. In this appendix, the impact force is considered as the only load on the HI-TRAC.

### 3.AN.2 HANDLING ACCIDENT - SIDE DROP

Handling accidents with a HI-TRAC transfer containing a loaded MPC are credible events only with HI-TRAC initially horizontal (Table 3.1.5). The stress analyses carried out in Chapter 3 of this safety analysis report assume that the inertial loading on the load bearing members of the MPC, the fuel basket, and the transfer cask due to a handling accident are limited by the Table 3.1.2 decelerations. The maximum deceleration experienced by a structural component is the product of the rigid body deceleration sustained by the structure and the dynamic load factor (DLF) applicable to that structural component. The dynamic load factor (DLF) is a function of the contact impulse and the structural characteristics of the component. A solution for dynamic load factors is provided in Appendix 3.X.

The rigid body deceleration is a strong function of the load-deformation characteristics of the impact interface, weight of the cask, and the drop height. For the HI-TRAC System, the weight of the structure and its surface compliance characteristics are known. However, the contact stiffness of the ISFSI pad (and other surfaces over which the HI-TRAC may be carried during its movement to the ISFSI) is site-dependent. The contact resistance of the collision interface, which is influenced by the HI-TRAC local compliance and the impacted surface compliance, therefore, is not known a priori for

a site. Analyses for the HI-TRAC body decelerations are presented here for a reference ISFSI pad (which is the pad used in a recent Lawrence Livermore National Laboratory report).

### 3.AN.2.2 Purpose

The purpose of this simulation is to demonstrate that the rigid body decelerations of the 125-ton and 100-ton HI-TRAC transfer casks are sufficiently low so that the design basis deceleration of 45g is not exceeded. Only one type of accidental drop (a side drop) of a loaded HI-TRAC transfer cask on the ISFSI pad is considered in this appendix. The loaded HI-TRAC, attached to the transfer lid, free-falls from a horizontal orientation (the transfer cask's longitudinal axis is horizontal) from a height "h", before impacting the horizontal target surface. The height, "h", is measured from the target surface up to the *lowest* point on the transfer cask system. For the side drop analyses in this appendix, "h", is

h = 42"

Two initial orientations for HI-TRAC are considered to bound the handling accident:

In scenario A, the cask impacts the target with the lowest point being the rotation trunnion. The cask has a primary impact between the lower rotation trunnion and the target pad and then a secondary impact between the water jacket and the upper trunnion and the target pad. Figure 3.AN.2 shows the orientation for this scenario after the end of the event.

In scenario B, the primary impact occurs between the transfer lid and the target pad with a secondary impact following between the water jacket and the pad. Figure 3.AN.1 shows the orientation for this scenario after the end of the event.

Scenario B, with the trunnions initially in a horizontal plane, represents the normal transfer orientation and maximizes the slapdown angle when secondary impact begins.

Scenario A, with the trunnions vertical, represents a handling accident where the transfer cask is assumed to rotate 90 degrees prior to target impact. This scenario insures that the rotation trunnion suffers a direct strike at primary impact and maximizes the potential for the involvement of the lifting trunnions in the secondary impact.

### 3.AN.2.3 Background and Methodology

The analysis of the HI-TRAC handling accident follows the similar analysis of the HI-STORM 100 accident evaluation. The methodology and the model is based on the work performed by Lawrence Livermore National Laboratory (LLNL) [3.AN.1, 3.AN.2]. Subsequently, USNRC personnel published a paper [3.AN.3] affirming the NRC's endorsement of the LLNL methodology. The LLNL simulation used modeling and simulation algorithms contained within the commercial computer code DYNA3D [3.AN.6].

Holtec has previously developed a finite element model for implementation on DYNA3D that is fully consistent with LLNL's cask model (including the use of the Butterworth filter for discerning rigid body deceleration from "noisy" impact data). The details of the DYNA3D dynamic model, as it has been applied to the HI-STAR 100 overpack are contained in a proprietary benchmark report [3.AN.4] wherein it is shown that the peak deceleration in every case of billet drop analyzed by LLNL is replicated within a small tolerance by the Holtec model. The case of the so-called "generic" cask, for which LLNL provided predicted response under side drop and tipover events, is also bounded by the Holtec model. In summary, the benchmarking effort documented in [3.AN.4] is in full compliance with the guidance of the Commission [3.AN.3].

Having developed and benchmarked an LLNL-consistent cask impact model, this model has been applied to prognosticate the HI-STAR 100 drop scenarios in a previous FSAR, and has been applied herein (see Appendix 3.A) to evaluate the HI-STORM 100 overpack performance during handling accidents.

In this section, the NRC approved target (reinforced concrete pad with underlying soil) is modeled together with the NRC approved MPC model. The HI-STORM 100 overpack is replaced with a finite element model of the HI-TRAC transfer cask. For the side drop scenario, considering the reference target (pad) elasto-plastic-damage characteristics, the object is threefold:

1. To demonstrate that the drop height "h" is such that the rigid body deceleration of the HI-TRAC, anywhere in the active fuel region, is below the 45g-design basis.
2. To demonstrate that the inner shell of the HI-TRAC does not suffer permanent deformation to the extent that ready retrievability of the contained MPC is compromised.
3. To demonstrate that global stresses in the HI-TRAC transfer cask, away from the impact interfaces, do not exceed the Level D stress intensities permitted by the ASME Code, Section III, Appendix F, for Class 3 NF components.

A description of the work effort and a summary of the results are presented in the following sections.

#### 3.AN.2.4            Assumptions and Input Data

##### 3.AN.2.4.1        Assumptions

The assumptions used to create the model are completely described in Reference [3.AN.4] and are shown there to be consistent with the LLNL simulation. There are two key aspects that are restated here:

The cask pad is assumed to be identical to the pad defined by LLNL [3.AN.2]. It is also identical to the pad utilized in the benchmark report [3.AN.4]. The essential data that defines the reference pad used to qualify the HI-TRAC System is provided in Table 3.AN.1.

#### 3.AN.2.4.2 Input Data

Table 3.AN.1 characterizes the properties of the reference target pad used in the analysis. The inputs are taken from References [3.AN.2] and [3.AN.4].

Table 3.AN.2 details the geometry of the 100-ton and 125-ton HI-TRAC used in the side drop simulations. This data is taken from applicable HI-TRAC drawings and Tables in Section 3.2.

#### 3.AN.2.5 Finite Element Models

Four finite-element models, corresponding to each of the postulated impact scenarios (A and B) pertinent to both types of casks (100-ton HI-TRAC and 125-ton HI-TRAC), are constructed using the pre-processor integrated with the DYNA3D software [3.AN.5]. A typical finite-element model is organized into 16 independent parts describing all structural components of the HI-TRAC System (the transfer lid plates, the bottom flange, the interior and exterior shell, the lead shielding, the top flange, the top lid, the lower and upper trunnions, the radial channels and outer closure plates of the water jacket), the MPC (steel plates and the basket fuel zone), and the concrete pad and the elastic soil stratum. Using symmetry, only a half finite-element model is constructed. The finite-element models used to numerically investigate the postulated side-drop scenarios are depicted in Figures 3.AN.3, 3.AN.4, and 3.AN.11.

The structural components of the HI-TRAC System are represented by elasto-plastic materials (\*MAT\_PIECEWISE\_LINEAR\_PLASTICITY), while the concrete pad and the soil stratum retain the material description used in the NRC approved HI-STAR 100 FSAR and also used in Appendix 3.A. for HI-STORM 100 overpack accident analyses.

The soil grid is a rectangular prism (800 inches long, 375 inches wide and 470 inches deep), and is constructed from 13294 solid type finite-elements. The material defining this part is an elastic orthotropic material. The central portion of the soil (400 inches long, 150 inches wide and 170 inches deep) where the stress concentration is expected to appear is discretized with a finer mesh.

The concrete pad is 320 inches long, 100 inches wide and is 36 inches thick. This part contains 8208 solid finite-elements. A uniform sized finite-element mesh is used to model the concrete pad. The concrete behavior is described using a special constitutive law and yielding surface (contained within DYNA3D). The geometry, the material properties, and the material behavior are identical to the LLNL reference pad.

The MPC and the contained fuel are modeled in two parts that represent the lid and baseplate, and the fuel area. An elastic material is used for both parts. The finite-element mesh pertinent to the MPC contains 1122 solid finite-elements. The MPC model is identical to that used in the cited handling accident simulations for the HI-STAR and HI-STORM overpacks. Gaps between the MPC and the transfer cask inner shell and lids are included in the model.

### 3.AN.2.6 Impact Velocity

For the side drop events, the impact velocity,  $v$ , is readily calculated from the Newtonian formula:

$$v = \sqrt{(2gh)}$$

where

$g$  = acceleration due to gravity  
 $h$  = free-fall height

The impact velocity, corresponding to a drop height of 42 inches, used in the numerical investigations presented in this appendix is 180.16 inch/second.

### 3.AN.2.7 Results

The DYNA3D deceleration time-history results are processed using a Butterworth filter (in conformance with the LLNL methodology and previously used in the HI-STAR 100 and HI-STORM 100 overpack analyses) to establish the rigid body deceleration of the HI-TRAC cask. All other outputs (displacements, forces) presented are directly (un-filtered) from the DYNA3D solver. A total of four simulations have been performed (2 casks with 2 initial orientations). The following "roadmap" summarizes the graphical results from the totality of simulations performed in support of the HI-TRAC transfer cask handling accident.

ITEM	HI-TRAC 125 – Scenario A	HI-TRAC 125 – Scenario B	HI-TRAC 100 – Scenario A	HI-TRAC 100 – Scenario B
Overall Model	Figure 3.AN.3	Figure 3.AN.11	-	-
HI-TRAC Mesh	Figure 3.AN.4	-	-	-
Z- Displacement at Transfer Lid, Top Lid	Figure 3.AN.5	Figure 3.AN.12	-	Figure 3.AN.20
Z- Deceleration at Centroid of Transfer Lid	Figure 3.AN.6	-	-	-
Z-Deceleration at Centroid of Inner Shell	Figure 3.AN.7	-	-	-
Z-Deceleration at Centroid of Top Lid	Figure 3.AN.8	-	-	-
Rigid Body Decelerations of Centroid of Transfer Lid, Inner Shell, and Top Lid	-	Figure 3.AN.13	Figure 3.AN.17	Figure 3.AN.21
Interface Force at Target/Primary and Secondary Impact Sites	Figure 3.AN.9	Figure 3.AN.14	Figure 3.AN.18	Figure 3.AN.22
Z-Displacements at Centroid of Inner Shell – Upper and Lower Points	Figure 3.AN.10	Figure 3.AN.15	Figure 3.AN.19	Figure 3.AN.23
Interface Force – Top Lid/MPC	-	Figure 3.AN.16	-	Figure 3.AN.24

Table 3.AN.3 presents the summary of all key results that are gleaned from the analyses. Within each data block in Table 3.AN.3, the specific figure number is given in parentheses. Where impact forces are reported in the tables, the reported value in Table 3.AN.3 has been doubled to reflect that the actual analysis model encompassed only one-half of the geometry. Table 3.AN.3 generally reports

peak values. However, there are three specific additional calculations that use the tabular results to derive additional information. In the section below, we demonstrate that:

1. The top lid never impacts the target.
2. The diametric change in the HI-TRAC inner shell diameter is such that the MPC retrievability is not compromised.
3. The interface force between the transfer lid and the HI-TRAC bottom flange can be computed from available data from the drop simulations.

To demonstrate that the top lid suffers no direct impact with the target, we examine the maximum vertical displacement of the top lid and the transfer lid (Figures 3.AN.5, 3.AN.12, and 3.AN.20). The allowable vertical displacement of the top lid (assuming no vertical displacement of the target pad) can be obtained from the drawings and bills-of-material for the HI-TRAC casks. Knowing the initial position of the lowest point on the top lid at the beginning of the event, we need only compare the allowable displacement plus any target pad displacement distance with the differential distance obtained from Figures 3.AN.5, 3.AN.12, and 3.AN.20. The following tabulation summarizes the results from inspection of the drawings and the figures:

ITEM	125-TON –Scenario A	125-TON Scenario B	100-TON Scenario B
Allowable Top Lid Vertical Displacement (from Drawings) Plus Target Vertical Deflection (inch)	-12.8469*	-28.77	-28.462
Top Lid Vertical Displacement (inch)	-9.75 (3.AN.5)	-27.3 (3.AN.12)	-27.5 (3.AN.20)
Transfer Lid Vertical Displacement (inch)	-2.0 (3.AN.5)	+1.0 (3.AN.12)	+2.25 (3.AN.20)
Maximum Angle of Inclination (Degrees)	2.31	8.46	8.93
Differential Vertical Displacement (inch)	-7.75	-28.3	-29.75

\* Vertical deflection of target not included in this table value.

An estimate for the local deformation of the target under the secondary impact location is obtained from Figures 3.AN.29 and 3.AN.30, for example, and is included in the allowable top lid displacement in the columns associated with “Scenario B”. These figures show the 100-ton HI-TRAC at the instant of maximum vertical deformation; the conclusion that the lid does not impact the target, as demonstrated in the table, is independently confirmed by Figure 3.AN.30. In the table above, the angle of inclination is computed as the angle whose “sin” is the differential vertical displacement divided by the distance between the measurement points (per Table 3.AN.2).

To demonstrate retrievability of the MPC, the change in the diameter of the inner shell of HI-TRAC can be computed from the DYNA3D output for absolute displacements of two opposing points on the

inner shell. Figure 3.AN.25 shows the geometry at the beginning of the event, and at a rotated position. The vertical movements  $V_T$  and  $V_B$  (a negative sign means displacement is toward target pad) are calculated by DYNA3D and shown in Figures 3.AN.10, 3.AN.15, 3.AN.19, and 3.AN.23. The rotation angle is computed in the tabulation above. The diametric decrease is  $|U_B - U_T|$  and is computed from the following formula:

$$|U_B - U_T| = \frac{|V_B - V_T| - D(1 - \cos(\theta))}{\cos(\theta)}$$

The following results are obtained using the results from DYNA3D and the preceding formula:

Maximum Change in Diameter of HI-TRAC from Secondary Impacts	
CASE	Diametric Change (inch)
125-Ton, Scenario A	0.228
125 Ton, Scenario B	0.113
100 Ton, Scenario B	0.067

The above diametric changes are less than the nominal gap (reduced by the thermal expansion effect calculated in Appendix 3.I). The above calculation, together with the fact that there is no evidence of global plastic straining of the inner shell at the end of the simulation, supports the conclusion that ready retrievability of the MPC is not impaired by the handling accident.

Finally, we outline the computation of the interface force between the HI-TRAC bottom flange and the transfer lid. Figure 3.4.29 in Section 3.4 shows a free-body of the transfer lid at primary impact. With reference to that figure, the equation of equilibrium is:

$$M_{TL} a_{TL} = F_I - G_I$$

where

$M_{TL}$  = the mass of the transfer lid

$a_{TL}$  = the time varying acceleration of the centroid of the transfer lid

$F_I$  = the time varying contact force at the interface with the target

$G_I$  = the time varying interface force at the bottom flange/transfer lid interface

Solving for the interface force give the result

$$G_I = F_I - M_{TL} a_{TL}$$

Using the appropriate transfer lid mass and acceleration, together with the target interface force at the limiting time instant, provides values for the interface force. Using results from Table 3.AN.3 and transfer lid bounding weights from Table 3.2.2 gives the following results for peak interface forces:

HI-TRAC BOTTOM FLANGE/TRANSFER LID INTERFACE FORCE	
CASE	INTERFACE FORCE (kips)
125-Ton, Scenario A	1,183
125-Ton, Scenario B	1,272
100-Ton, Scenario A	1,129
100-Ton, Scenario B	1,070

Finally, we note that decelerations obtained from the DYNA3D numerical solutions are filtered through a Butterworth type filter identical to the filter used by LLNL to investigate the "generic" cask [3.AN.2]. The filter has the following characteristics: 350 Hz passband frequency, 10,000 Hz stopband frequency, 0.15 maximum passband ripple, and 10 minimum stopband attenuation.

The computer code utilized in this analysis is LS-DYNA3D [3.AN.5] validated under Holtec's QA system.

### 3.AN.3 LARGE TORNADO MISSILE IMPACT

#### 3.AN.3.1 Model

The finite element model used in the side drop analysis is used with the following modifications:

- a. The target is eliminated from the model and the HI-TRAC is restrained at the ends to equilibrate any applied missile impact force.
- b. The large tornado missile impact is simulated by a total input force-time relationship applied at nodes encompassing an interface area on the water jacket. The total force is apportioned to the nodes lying within and on the boundary of the interface area. The force-time relation is obtained from a NRC approved topical report [3.AN.7]. The interface contact area, appropriate to the large missile, is obtained from [3.AN.8]. The force-time relation (during the rise to a maximum value), is given by the expression [3.AN.7, Equation. D-6]:

$$F(t) = 0.625V_s W_m \sin(20t)$$

$$V_s = 184.6 \text{ ft./sec.}$$

$$W_m = 3960 \text{ lb.}$$

The time "t" in the formula is in "seconds".

Figure 3.AN.26 shows the interface force-time data imposed on the HI-TRAC water jacket. The interface area was assumed approximately mid-way along the length of the cask.

### 3.AN.3.2 Results from Analysis

Figures 3.AN.27 and 3.AN.28 show the Von Mises stress distribution in the water jacket for both HI-TRAC transfer casks at the instant when the applied interface force peaks. Table 3.AN.4 summarizes results from these figures as well as the strain data from the two simulations. No plastic strain occurs in the inner shell due to the impact in either simulation.

### 3.AN.4 COMPUTER CODES AND ARCHIVAL INFORMATION

The input and output files created to perform the analyses reported in this appendix are listed for future retrievability.

The computer code utilized in this analysis is DYNA3D [3.AN.5] validated under Holtec's QA system.

The DYNA3D computer code has an extensive finite-element and material description library and can account for various time-dependent contact conditions that normally arise between the various structural components during the impact analysis.

The input and the output files created are stored on Holtec's server disk and tape archived as required by Holtec's QA procedures under the following address:

F:\PROJECTS\5014\HITRAC\...

Each one of the subdirectories contains specific data related to the analyzed drop scenarios and is organized in five files: DYNA3D input file (XXX.DYN), corresponding to the analyzed drop event, and four time-history files (MATSUM- the impactor velocity time-history, RCFORC- the impact force time-history, NODOUT- displacement, velocity and acceleration and PLOT- the model deformation time-history) generated during the numerical analysis.

All DYNA3D simulations were performed in a PC environment (Windows 98), using a Dell Corporation Pentium II - 450 MHz computer.

### 3.AN.5 CONCLUSIONS

The DYNA3D analysis of HI-TRAC reported in this appendix leads to the following conclusions:

- a. If a loaded HI-TRAC, with its longitudinal axis horizontal, undergoes a free fall for a height of 42 inches and impacts a reference pad defined by Table 3.AN.1, the maximum rigid body deceleration at primary or secondary impact is below the design basis of 45g's. Therefore, since the design basis deceleration is 45 g', it is concluded that there will be no adverse effect on the fuel basket, within the MPC, by this handling accident.

- b. The maximum stress intensity in the HI-TRAC transfer cask is below Level D allowables during the side drop event and during the impact by a large tornado missile.
- c. The diametric change of the HI-TRAC inner shell is less than the minimum gap between the MPC and the inner shell of the HI-TRAC transfer cask. Therefore, after either a side drop or an impact by a large tornado missile, ready retrievability of the MPC is not adversely affected.

Tables 3.AN.3 and 3.AN.4 provide key results for all drop cases studied herein with additional results provided within the discussion.

### 3.AN.6 REFERENCES

- [3.AN.1] Witte, M., et al., "Evaluation of Low-Velocity Impacts Tests of Solid Steel Billet onto Concrete Pads.", Lawrence Livermore National Laboratory, UCRL-ID-126274, Livermore, California, March 1997.
- [3.AN.2] Witte, M., et al., "Evaluation of Low-Velocity Impacts Tests of Solid Steel Billet onto Concrete Pads, and Application to Generic ISFSI Storage Cask for Tipover and Side Drop.", Lawrence Livermore National Laboratory, UCRL-ID-126295, Livermore, California, March 1997.
- [3.AN.3] Tang, D.T., Raddatz, M.G., and Sturz, F.C., "NRC Staff Technical Approach for Spent Fuel Cask Drop and Tipover Accident Analysis", SFPO, USNRC (1997).
- [3.AN.4] Simulescu, I., "Benchmarking of the Holtec LS-DYNA3D Model for Cask Drop Events", Holtec Report HI-971779, September 1997.
- [3.AN.5] LS-DYNA3D, Version 936-03, Livermore Software Technology Corporation, September 1996.
- [3.AN.6] Whirley, R.G., "DYNA3D, A Nonlinear, Explicit, Three-Dimensional Finite element Code for Solid and Structural Mechanics - User Manual.", Lawrence Livermore National Laboratory, UCRL-MA-107254, Revision 1, 1993.
- [3.AN.7] Design of Structures for Missile Impact, BC-TOP-9A, Revision 2, Bechtel Power Corporation Topical Report, September, 1974.
- [3.AN.8] Missiles Generated by Natural Phenomena, NUREG-0800, SRP 3.5.1.4.

Table 3.AN.1: Essential Variables to Characterize the Reference Target

Thickness of concrete	36 inches
Nominal compressive strength of concrete	4,200 psi
Concrete mass density	2.097E-04 lb-sec <sup>2</sup> /in <sup>4</sup>
Concrete shear modulus	1.514E+06 psi
Concrete Poisson's ratio	0.22
Mass density of the engineered fill (soil)	1.498E-04 lb-sec <sup>2</sup> /in <sup>4</sup>
Modulus of elasticity of the soil	28,000 psi
Poisson's ratio of the soil	0.3

Note: The concrete Young's Modulus is derived from the American Concrete Institute recommended formula  $57,000\sqrt{f}$  where  $f$  is the nominal compressive strength of the concrete (psi).

Table 3.AN.2: Key Cask Input Data in Analyses

ITEM	HI-TRAC -125	HI-TRAC – 100
Total HI-TRAC Weight	152,636 lb.	109,214 lb.
Lead Weight	79,109 lb.	49,810 lb.
Overall Length of the Transfer Cask	207.875 inches	204.125 inches
Length x Width of Transfer Lid*	128 in. x 93 in.	128 in. x 89 in.
Outside Diameter of the Radial Channels	94.625 inches	91.0 inches
Inner Shell Diameter	68.75 inches	68.75 inches
Outer Radius of Top Lid	40.625 inches	39.0 inches
Longitudinal Distance Between Point on Transfer Lid and Point on Top Lid where Vertical Displacements are measured (inch)	192.25 inches	191.60 inches
MPC Weight (including fuel)	88,857 lb.	88,857 lb.
MPC Height	190.5 inches	190.5 inches
MPC Diameter	68.375 inches	68.375 inches
MPC Bottom Plate Thickness	2.5 inches	2.5 inches
MPC Top Plate Thickness	9.5 inches	9.5 inches

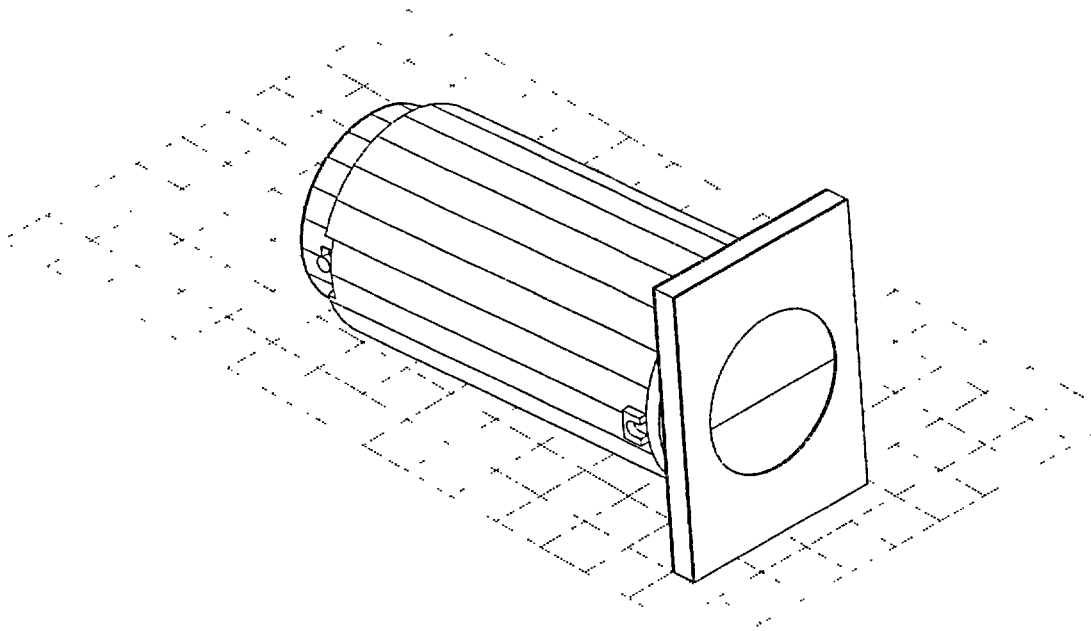
\* We note that the intermediate plate extends 2” beyond the length and provides the initial site for impact for the “Scenario B” orientation.

Table 3.AN.3: Side Drop Analyses Results

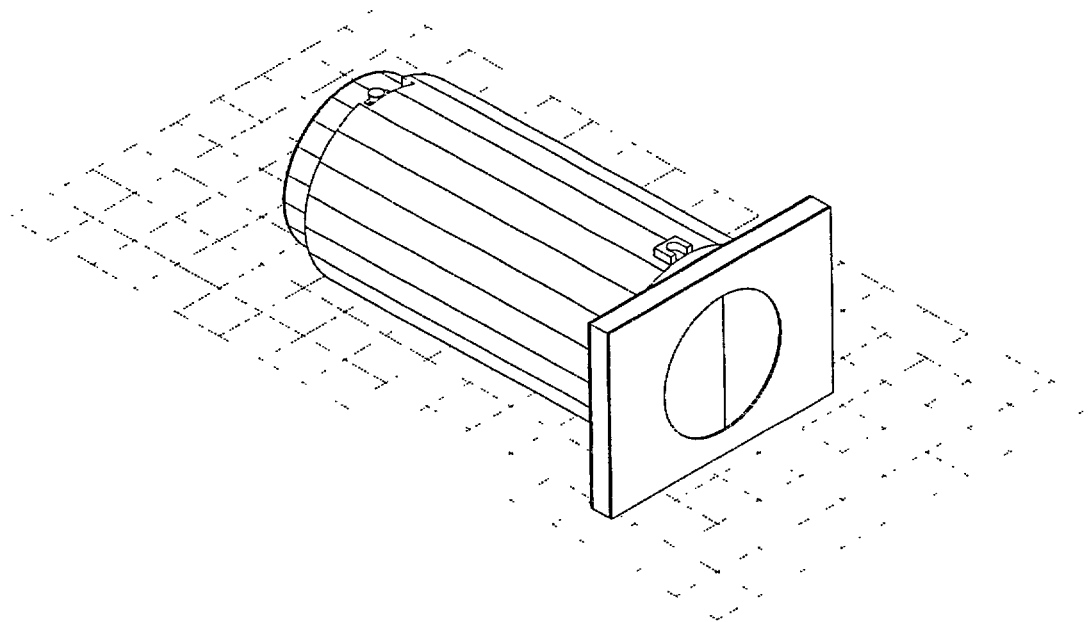
ITEM	HI-TRAC 125 – Scenario A	HI-TRAC 125 – Scenario B	HI-TRAC 100 – Scenario A	HI-TRAC 100 – Scenario B
Maximum Vertical Deceleration during Primary Impact (g's) – Transfer Lid	23.5 (3.AN.6)	30.8 (3.AN.13)	31.75 (3.AN.17)	35.0 (3.AN.21)
Vertical Deceleration at Top Lid at Instant of Max. g's Primary Impact (g's)	-1.0 (3.AN.8)	-9.0 (3.AN.13)	-3.0 (3.AN.17)	-8.0 (3.AN.21)
Max. Interface Force Target/Primary Impact Site (kips)	1,700 (3.AN.9)	1,950 (3.AN.14)	1,700 (3.AN.18)	1,700 (3.AN.22)
Maximum Vertical Deceleration at Centroid – Instant of Maximum Primary Impact Force on Target(g's)	6.0 (3.AN.7)	7.0 (3.AN.13)	12.5 (3.AN.17)	7.0 (3.AN.21)
Vertical Deceleration of Transfer Lid at Instant of Max. g's Secondary Impact (g's)	6.25 (3.AN.6, 3.AN.8)	-3.0 (3.AN.13)	-3.5 (3.AN.17)	-7.0 (3.AN.21)
Maximum Vertical Deceleration at Top Lid - Secondary Impact (g's)	32.0 (3.AN.8)	25.5 (3.AN.13)	45.0 (3.AN.17)	36.5 (3.AN.21)
Vertical Deceleration at Centroid at Instant of Max. g's Secondary Impact (g's)	13 (3.AN.7, 3.AN.8)	9.0 (3.AN.13)	17.5 (3.AN.17)	10.0 (3.AN.21)
Max. Interface Force Target/Secondary Impact Site (kips)	1,850 (3.AN.9)	1,300 (3.AN.14)	1,450 (3.AN.18)	1,500 (3.AN.22)
Max. Von Mises Stress (ksi)	38.367	37.577	40.444	40.690
Inner Shell Plastic Strain	0.002818	0.001146	0.006631	0.00492
Maximum MPC/Top Lid Interface Force (kips)	-	132 (3.AN.16)	-	39.0 (3.AN.24)
Max. Difference in Absolute Vertical Displacement of Opposing Points on Inner Shell (inch)	0.27 (3.AN.10)	0.5 (3.AN.15)	0.55 (3.AN.19)	1.1 (3.AN.23)

Table 3.AN.4 Large Tornado Missile Impact Analysis Results

ITEM	CALCULATED VALUE -125 TON	CALCULATED VALUE - 100 TON	ALLOWABLE VALUE
Maximum Stress Intensity in Water Jacket (ksi)	19.073	28.331	58.7
Maximum Stress Intensity in Inner Shell (ksi)	6.023	11.467	58.7
Maximum Plastic Strain in Water Jacket	0.0	0.0000932	-
Maximum Plastic Strain in Inner Shell	0.0	0.0	-



**FIGURE 3.AN.1; HI-TRAC TRANSFER CASK IN SHORT-SIDE IMPACT  
(CASK RESTS AT A POSITION OF  $-5^{\circ}$  FROM HORIZONTAL)**



**FIGURE 3.AN.2; HI-TRAC TRANSFER CASK IN LONG-SIDE IMPACT  
(CASK RESTS AT A POSITION OF  $-1^{\circ}$  FROM HORIZONTAL)**

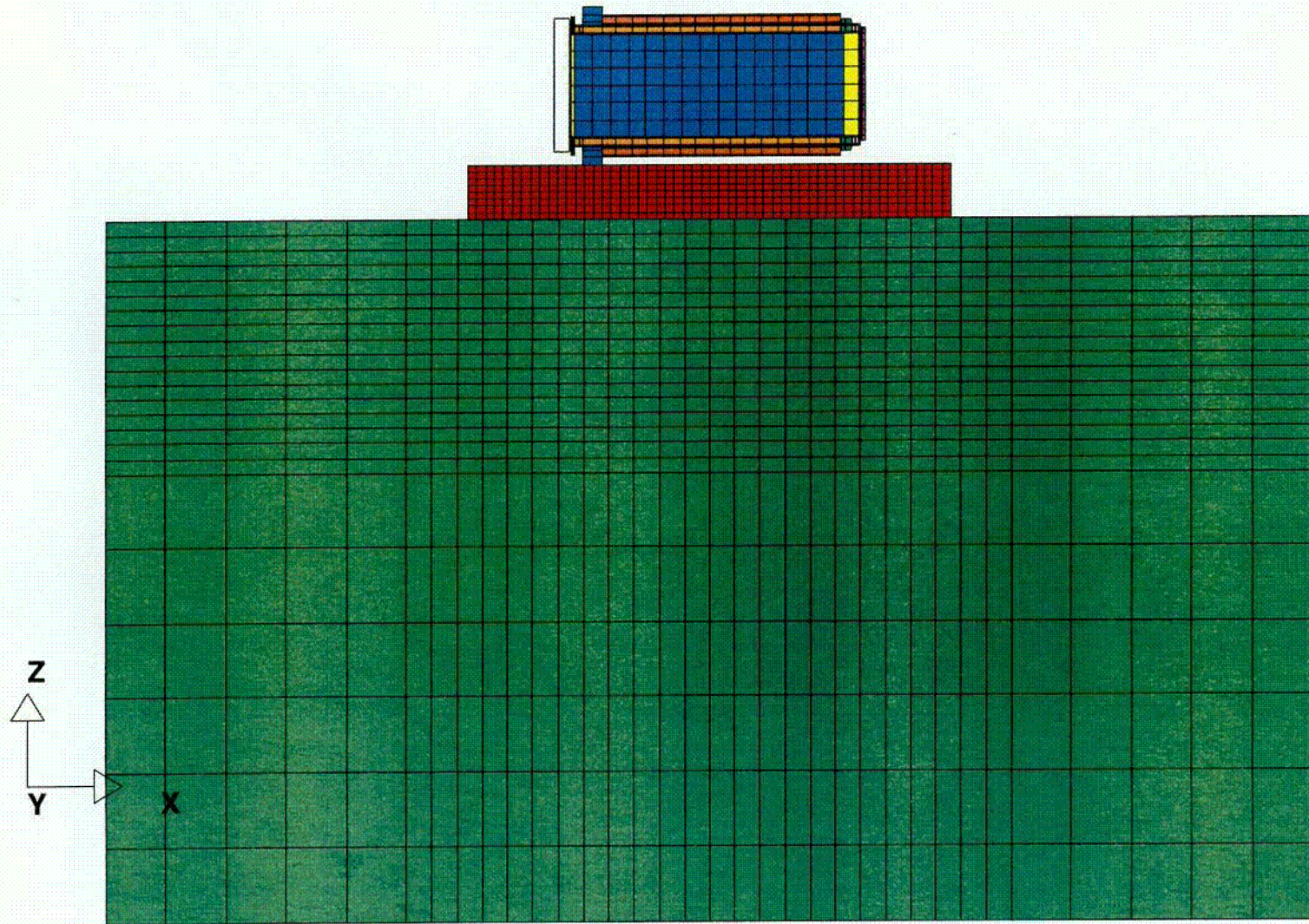


Figure 3.AN.3 125-ton High Trac, Scenario A

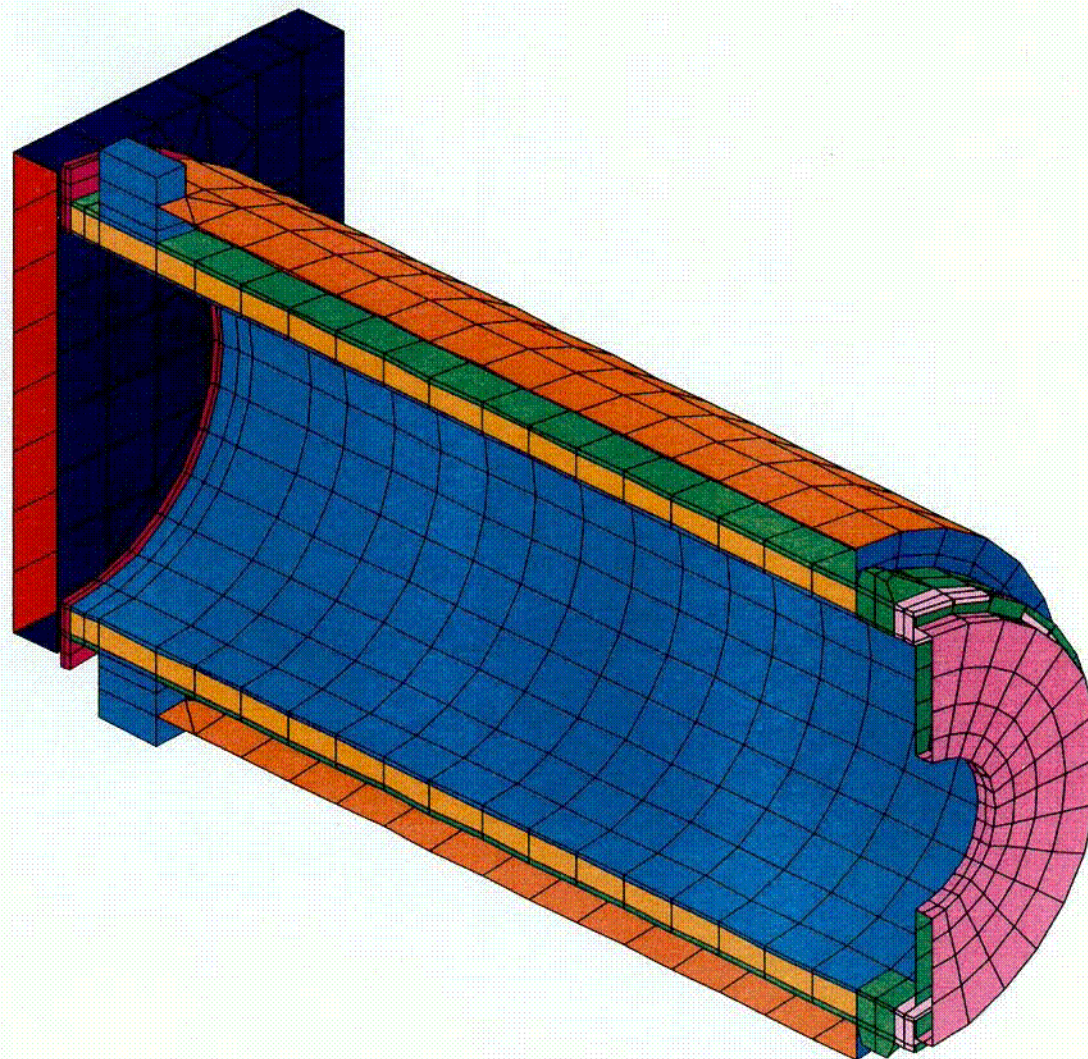
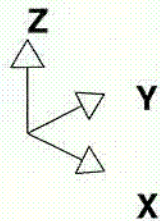
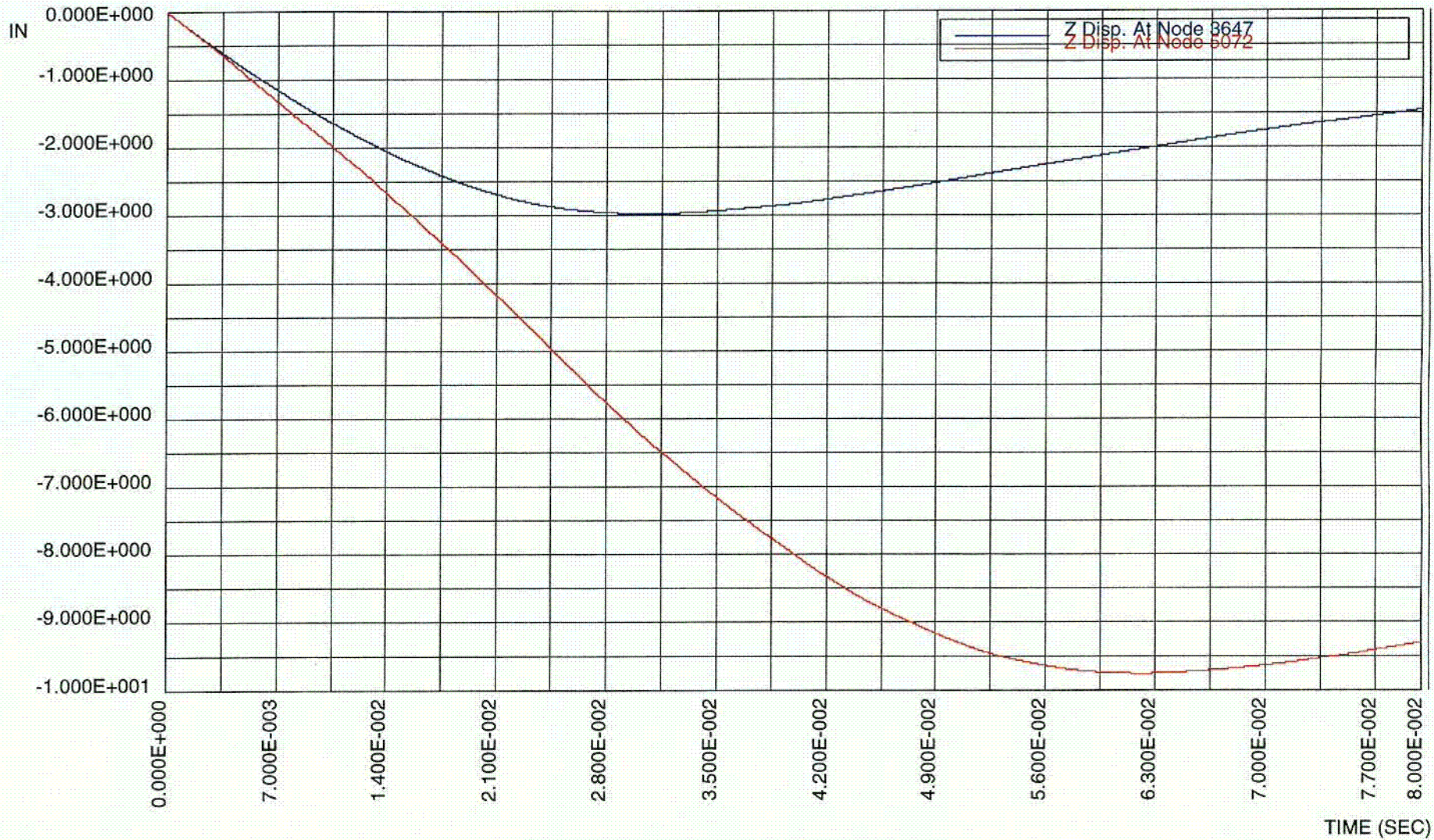


Figure 3.AN.4 HI TRAC 125 Finite Element Mesh

COZ

HI-STORM FSAR  
HI-2002444

Rev. 0

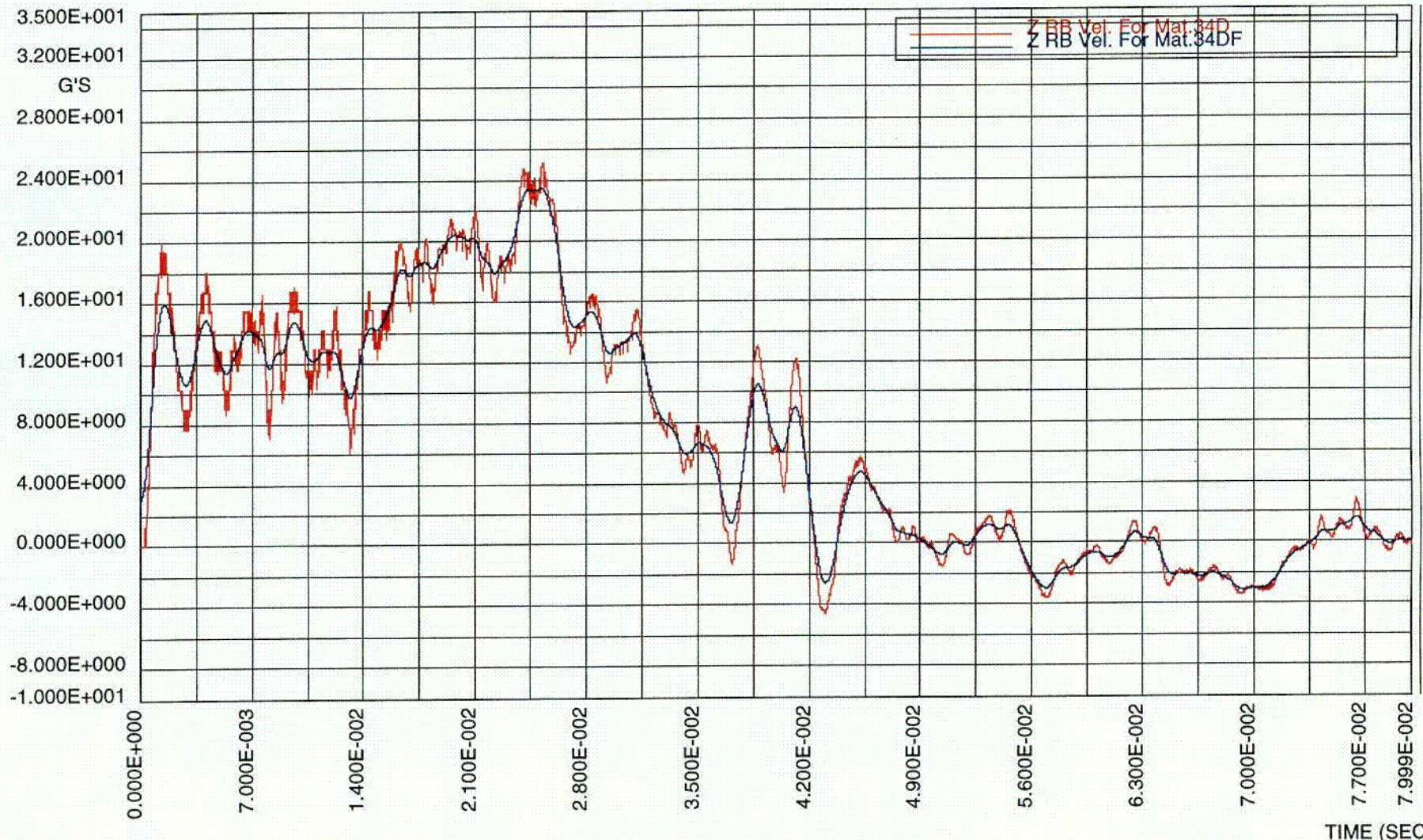


nodout: 125 HI-TRACK V0=180.16 IN/SEC ESOIL=28 KSI

Figure 3.AN.5 Vertical Displacement at Transfer Lid, Top Lid Outer Points, Scenario A

203  
 HI-STORM FSAR  
 HI-2002444

Rev. 0



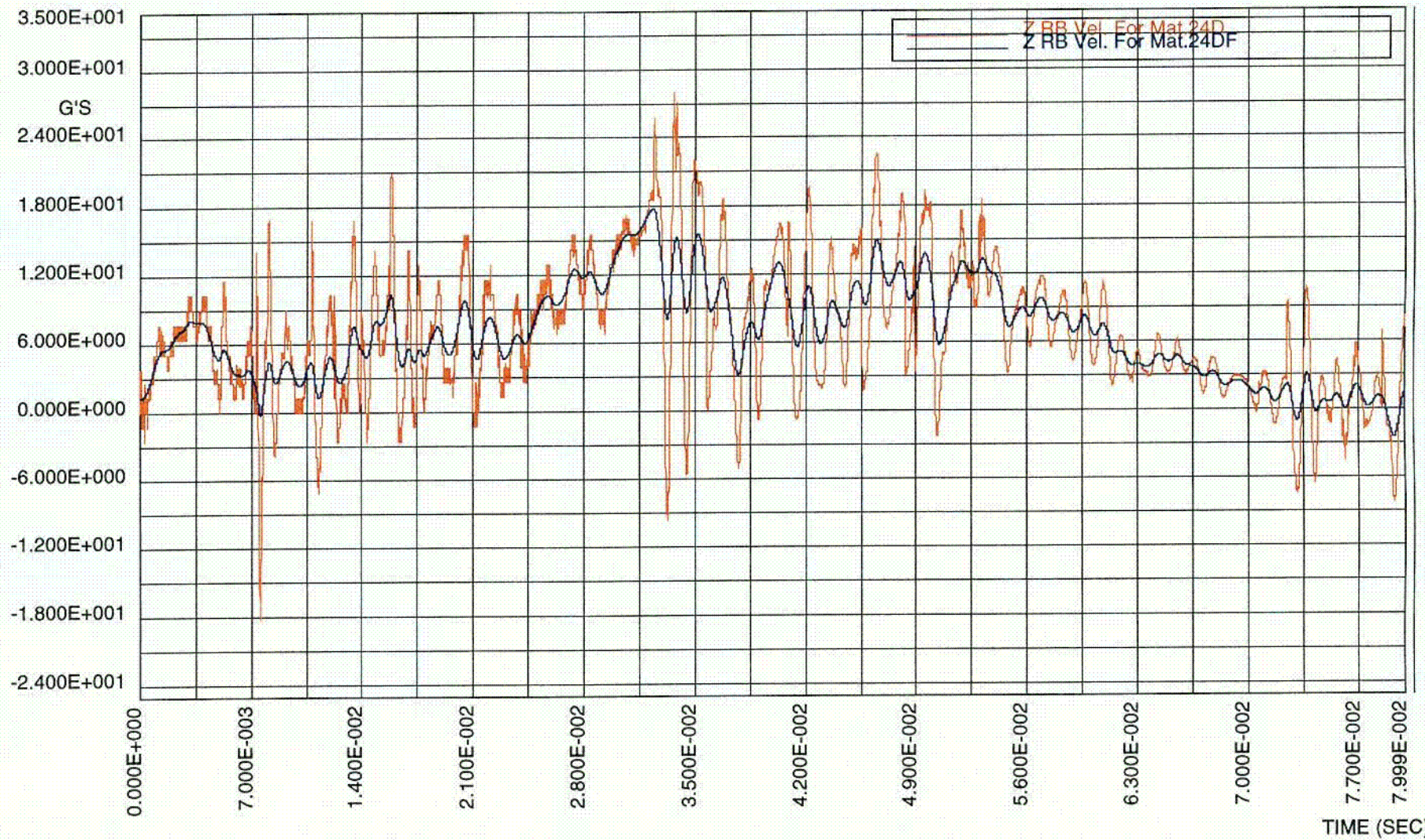
matsum: 125 HI-TRACK V0=180.16 IN/SEC ESOIL=28 KSI

Figure 3.AN.6 Vertical Deceleration at Transfer Lid, Scenario A

copy

HI-STORM FSAR  
HI-2002444

Rev. 0



matsum: 125 HI-TRACK V0=180.16 IN/SEC ESOIL=28 KSI

HI-STORM FSAR

Figure 3.AN.7 Vertical Deceleration at Inner Shell Centroid, Scenario A

HI-2002444

005

REV. 0

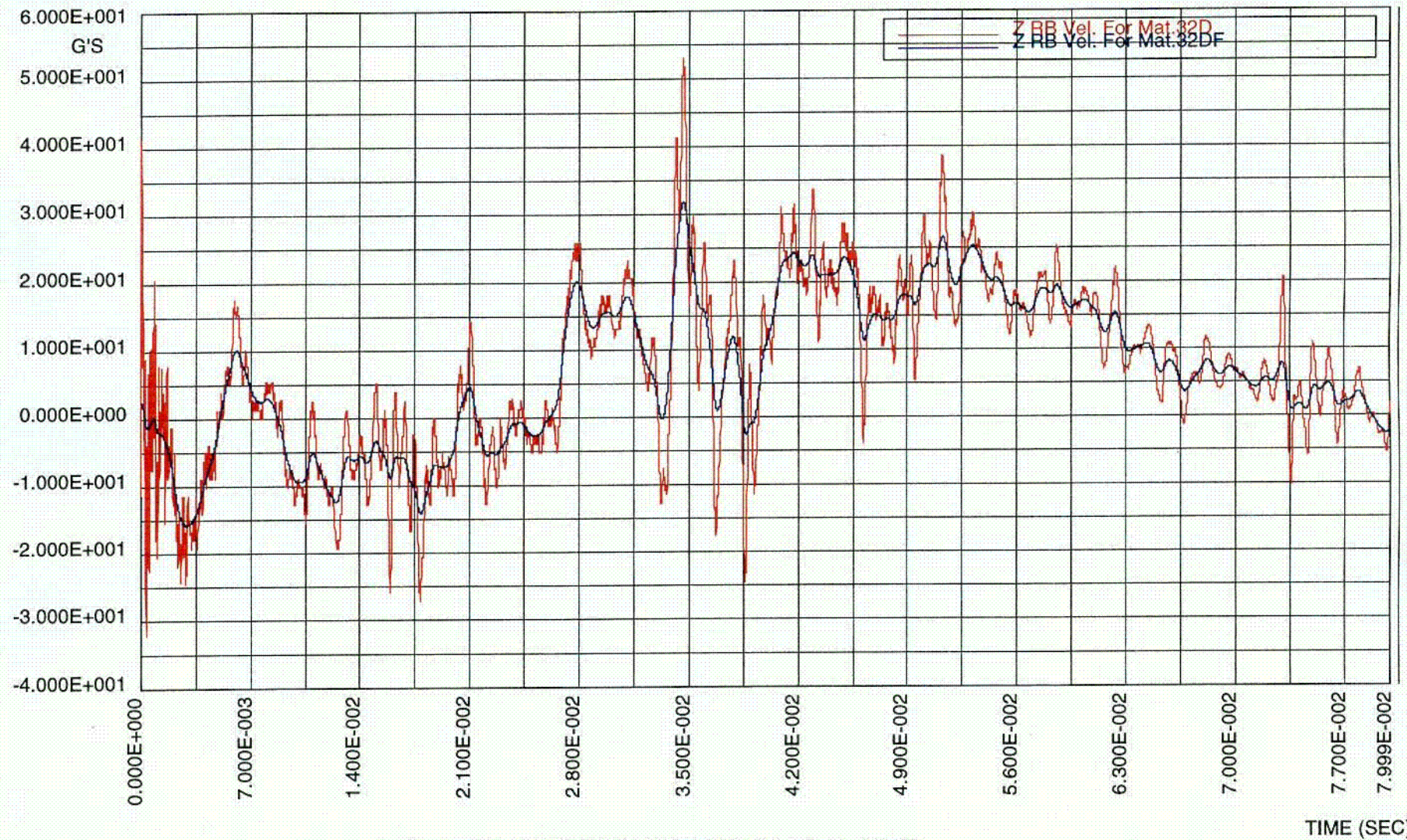
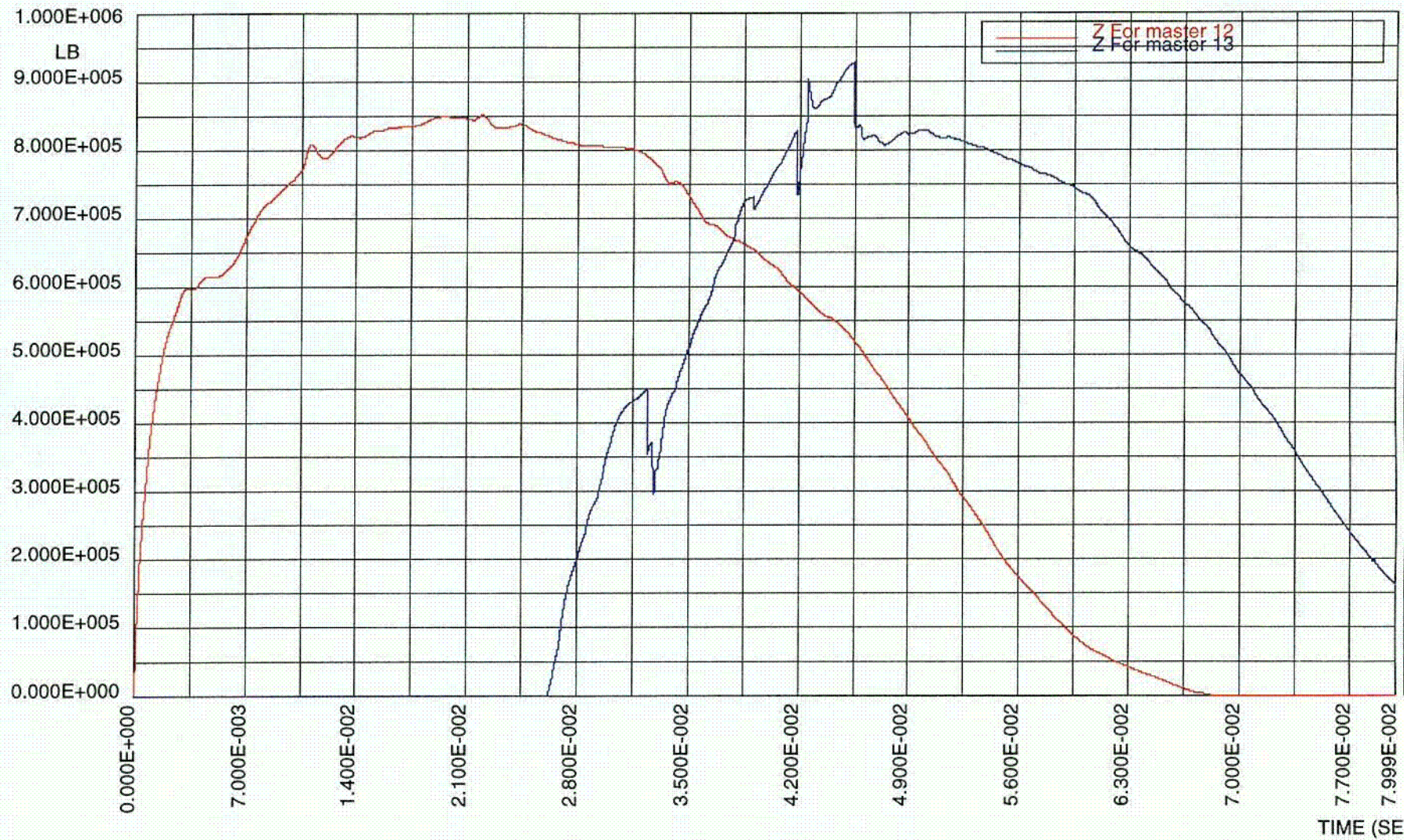


FIGURE 3.AN.8 VERTICAL DECELERATION OF TOP LID, SCENARIO A.

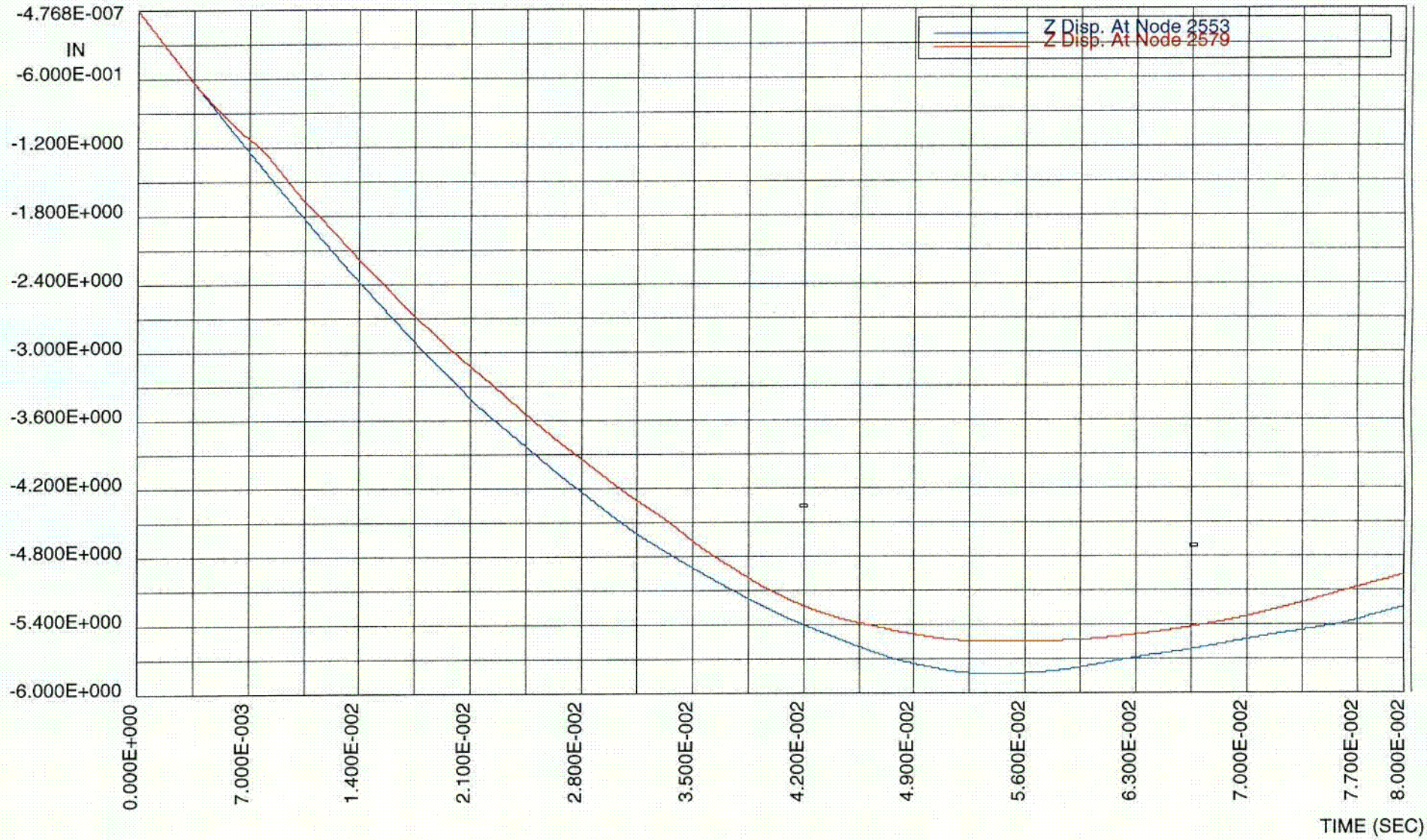


rcforc: 125 HI-TRACK V0=180.16 IN/SEC ESOIL=28 KSI

FIGURE 3.AN.9 INTERFACE FORCES AT TARGET/PRIMARY AND SECONDARY IMPACT SITES

LO7  
 HI-STORM FSAR  
 HI-2002444

Rev. 0



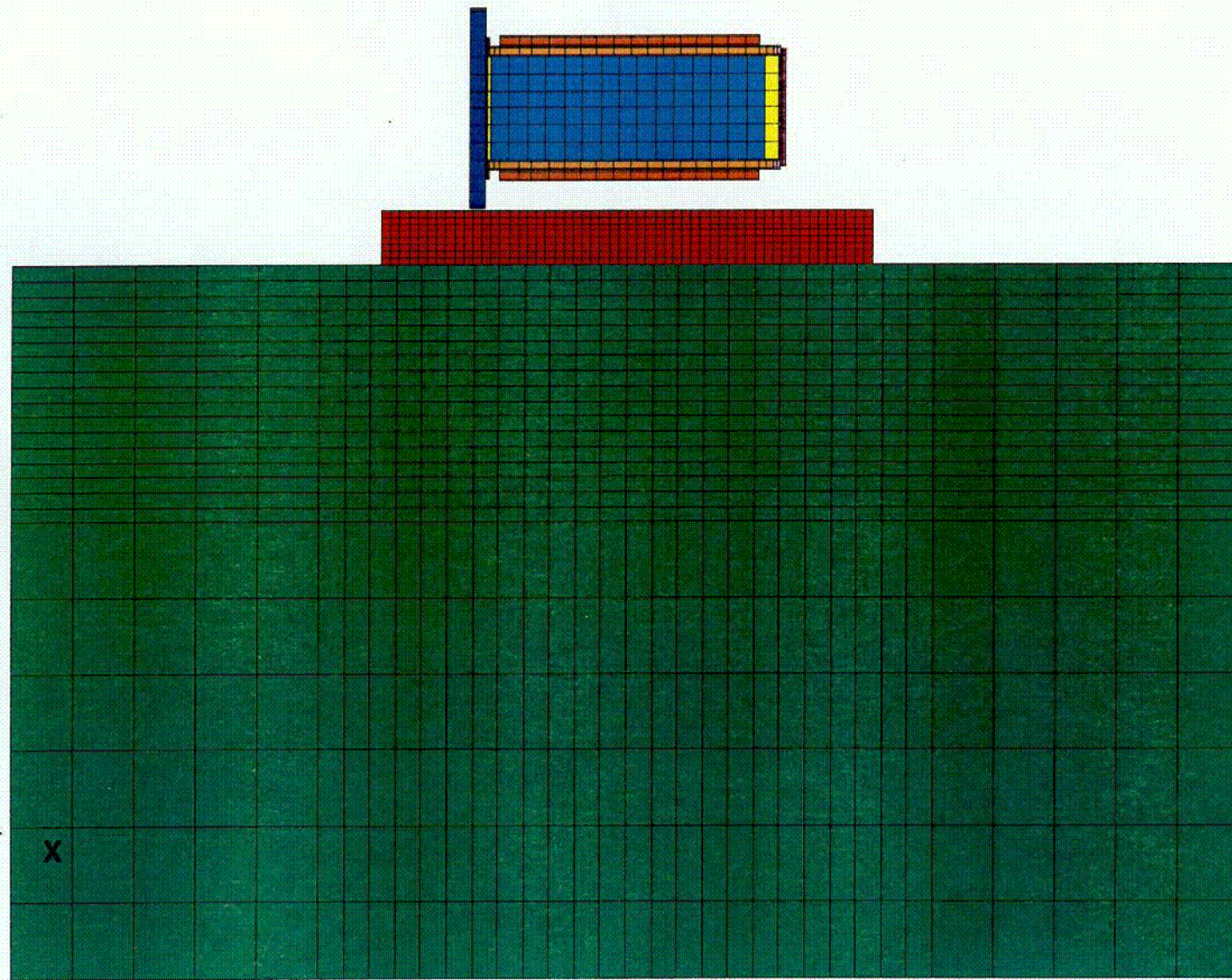
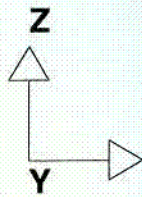
nodout: 125 HI-TRACK V0=180.16 IN/SEC ESOIL=28 KSI

FIGURE 3.AN.10: ABSOLUTE VERTICAL DISPLACEMENT AT CENTROID LOCATION (TOP AND BOTTOM OF INNER SHELL)

HI-STORM FSAR  
HI-2002444

REV. 0

800

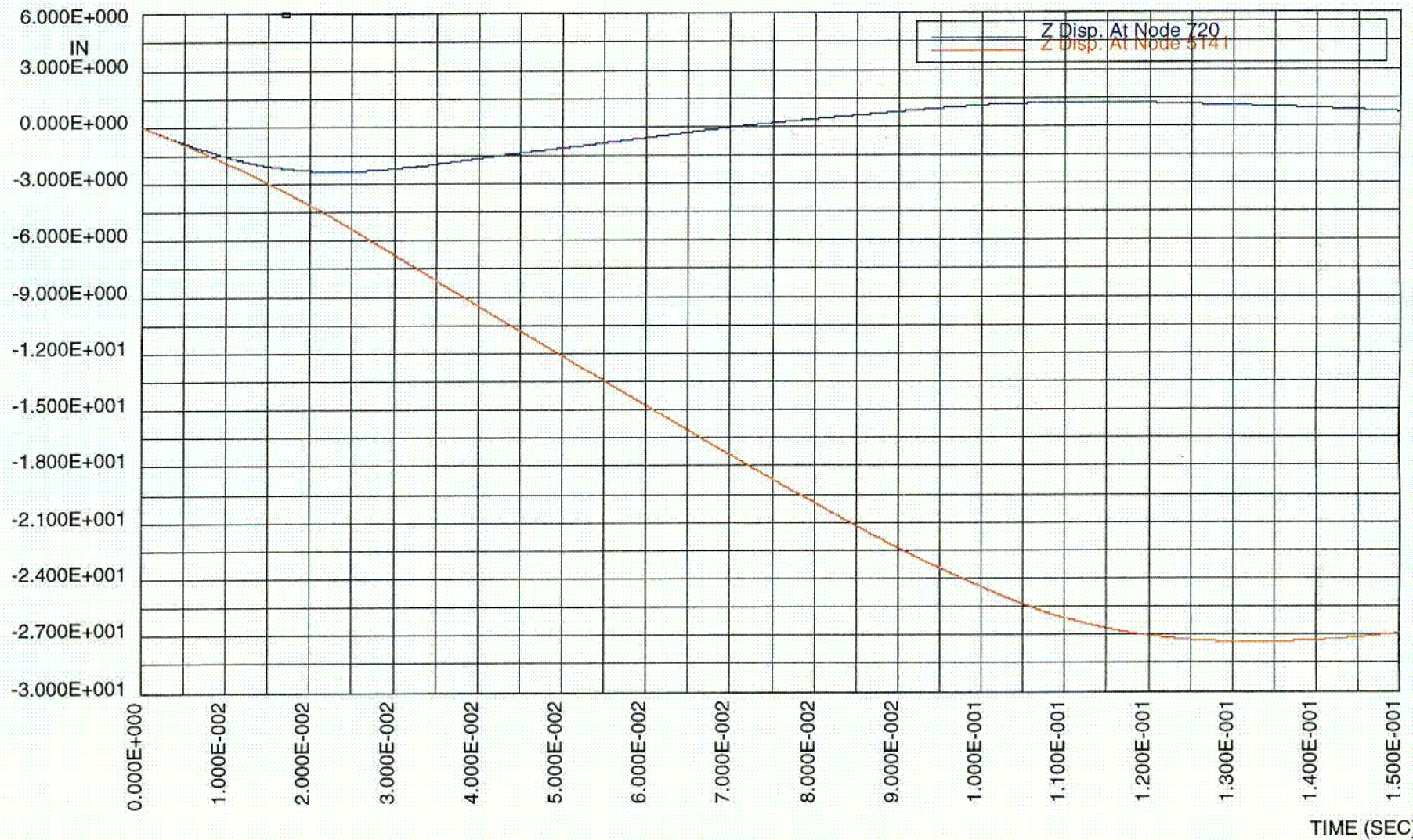


CO9

HI-STORM FSAR  
HI-2002444

FIGURE 3.AN.II; OVERALL MODEL OF 125 TON DROP, SCENARIO B

Rev. 0



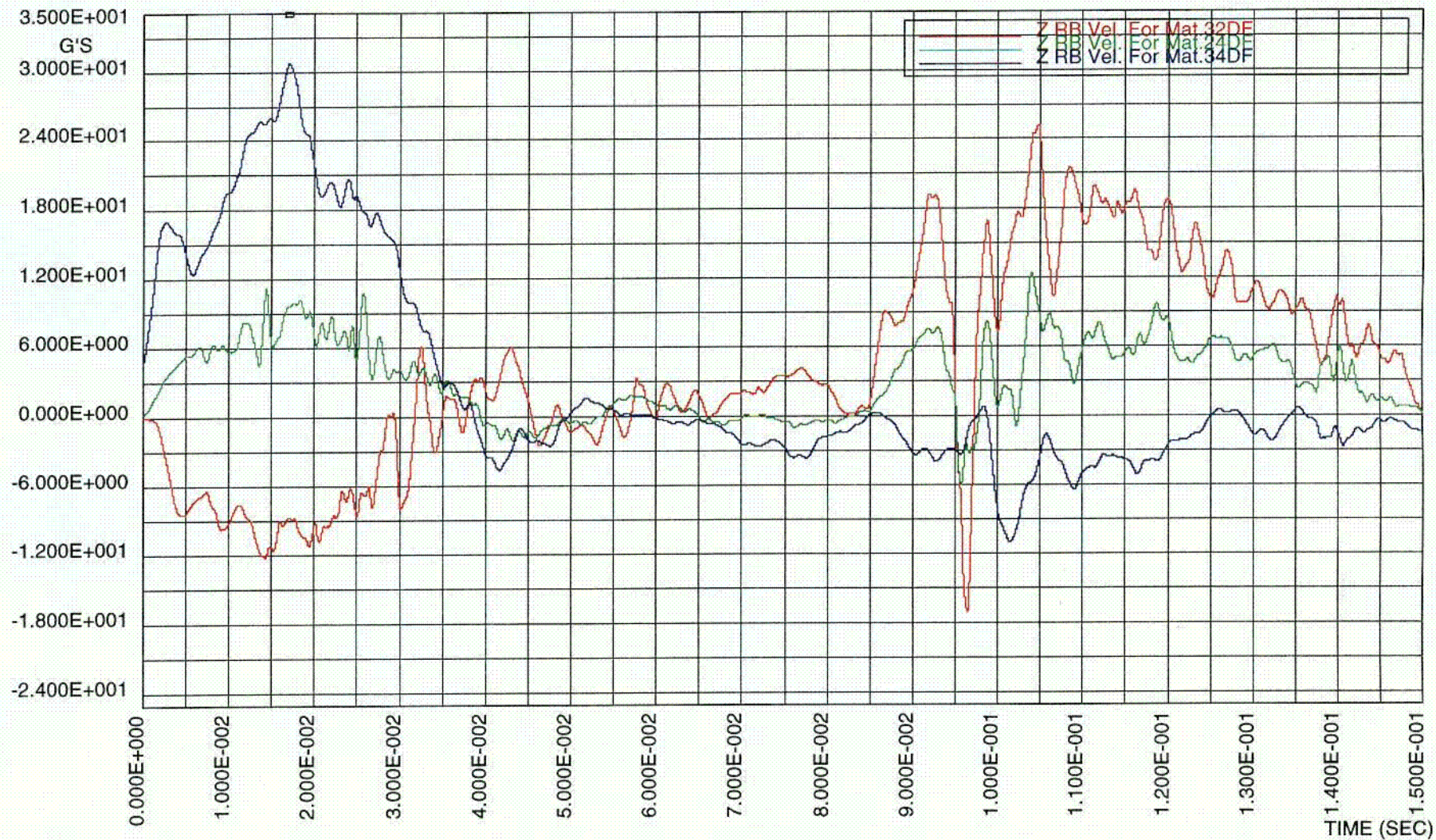
nodout: 125 HI-TRACK V0=180.16 IN/SEC ESOIL=28 KSI

FIGURE 3.AN.12; ABSOLUTE VERTICAL DISPLACEMENT AT TRANSFER LID AND TOP LID

C10

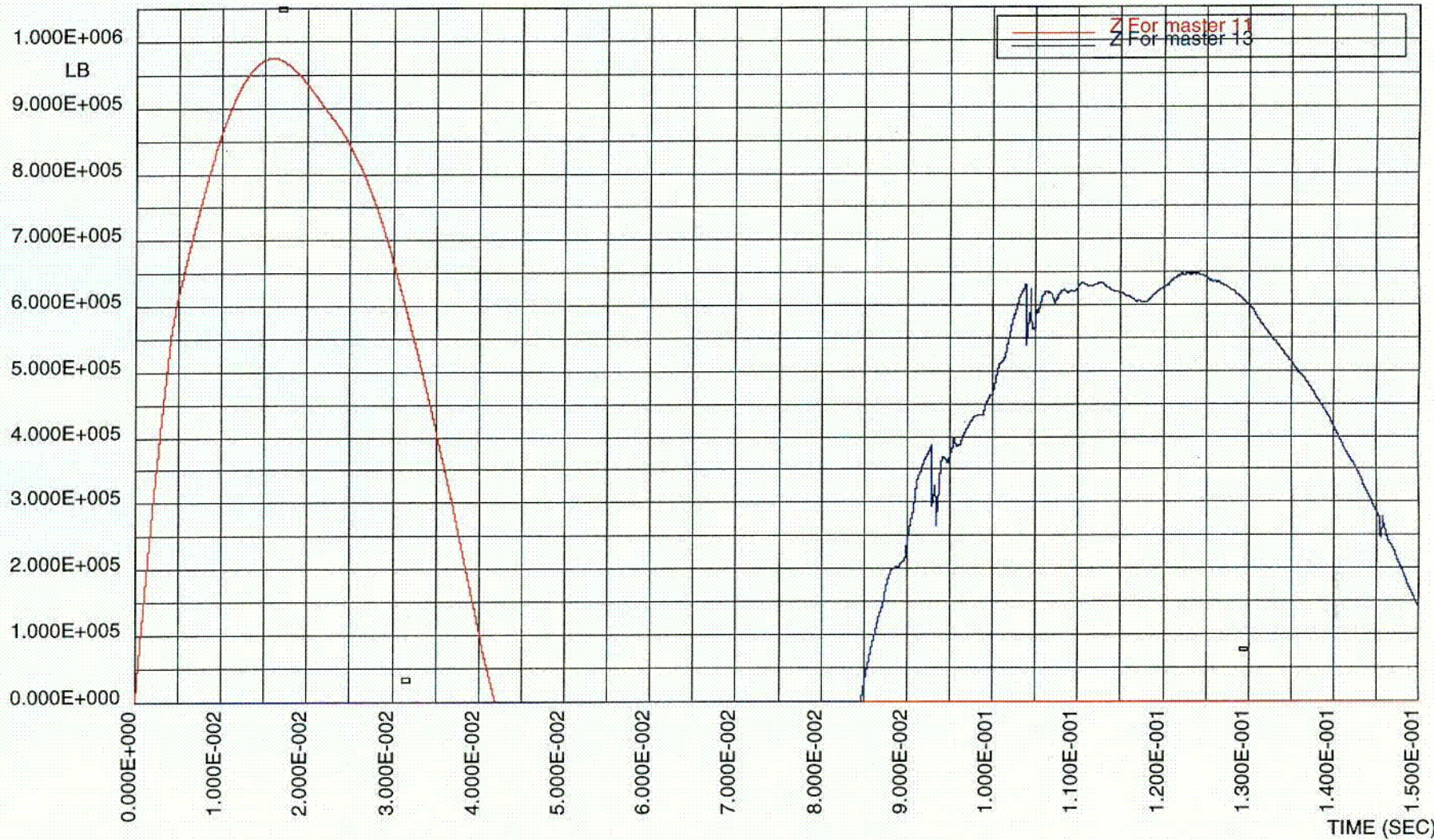
HI-STORM FSAR  
HI-2002444

Rev. 0



matsum: 125 HI-TRACK V0=180.16 IN/SEC ESOIL=28 KSI

FIGURE 3.AN.13; RIGID BODY DECELERATION-TRANSFER LID, CENTROID, TOP LID, SCENARIO B



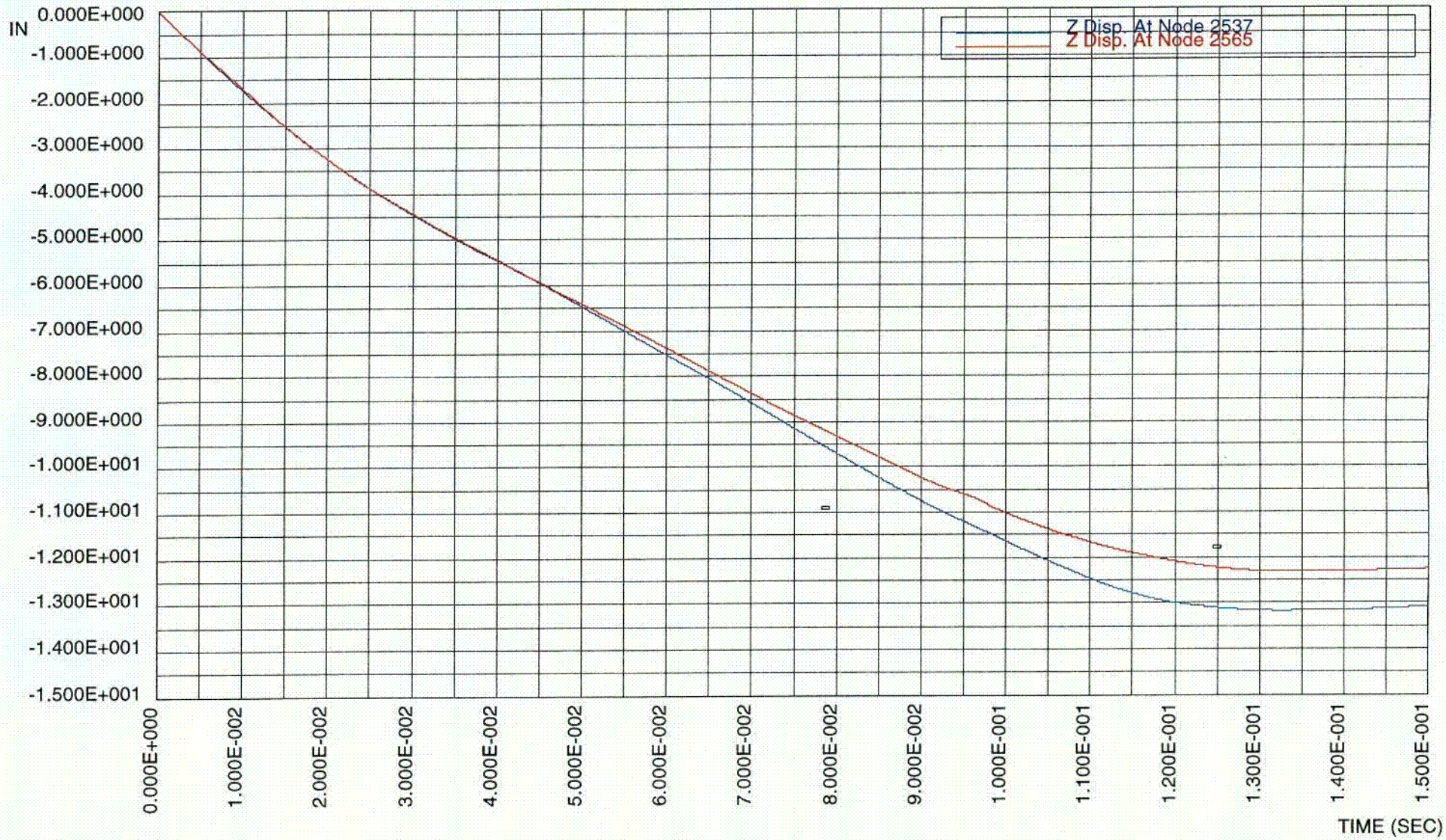
rcforc: 125 HI-TRACK V0=180.16 IN/SEC ESOIL=28 KSI

FIGURE 3.AN.14; INTERFACE FORCE ON TARGET, SCENARIO B

212

HI-STORM FSAR  
HI-2002444

Rev. 0



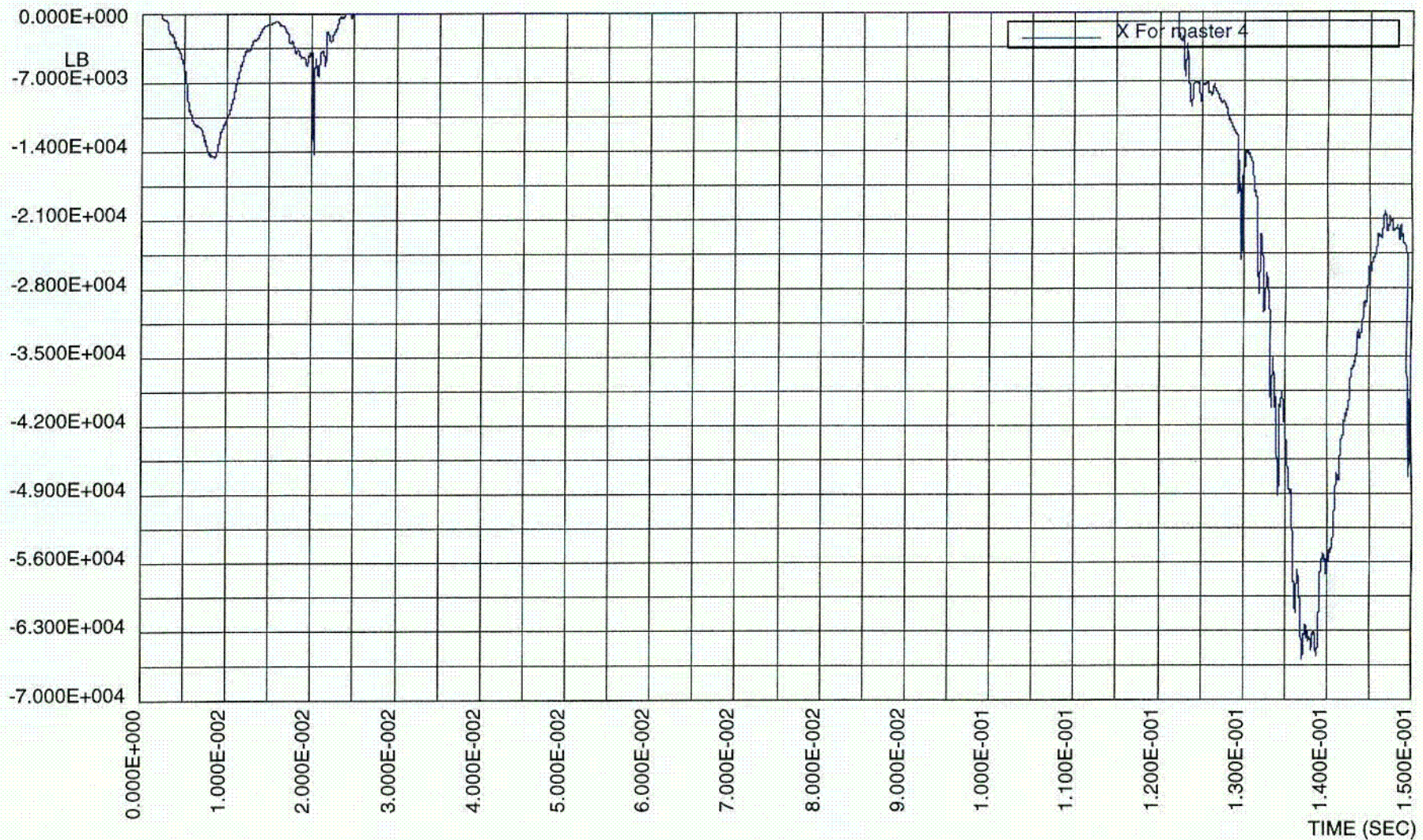
nodout: 125 HI-TRACK V0=180.16 IN/SEC ESOIL=28 KSI

FIGURE 3.AN.15; VERTICAL DISPLACEMENTS AT TOP AND BOTTOM OF INNER SHELL, SCENARIO B

HI-STORM FSAR  
HI-2002444

Rev. 0

313



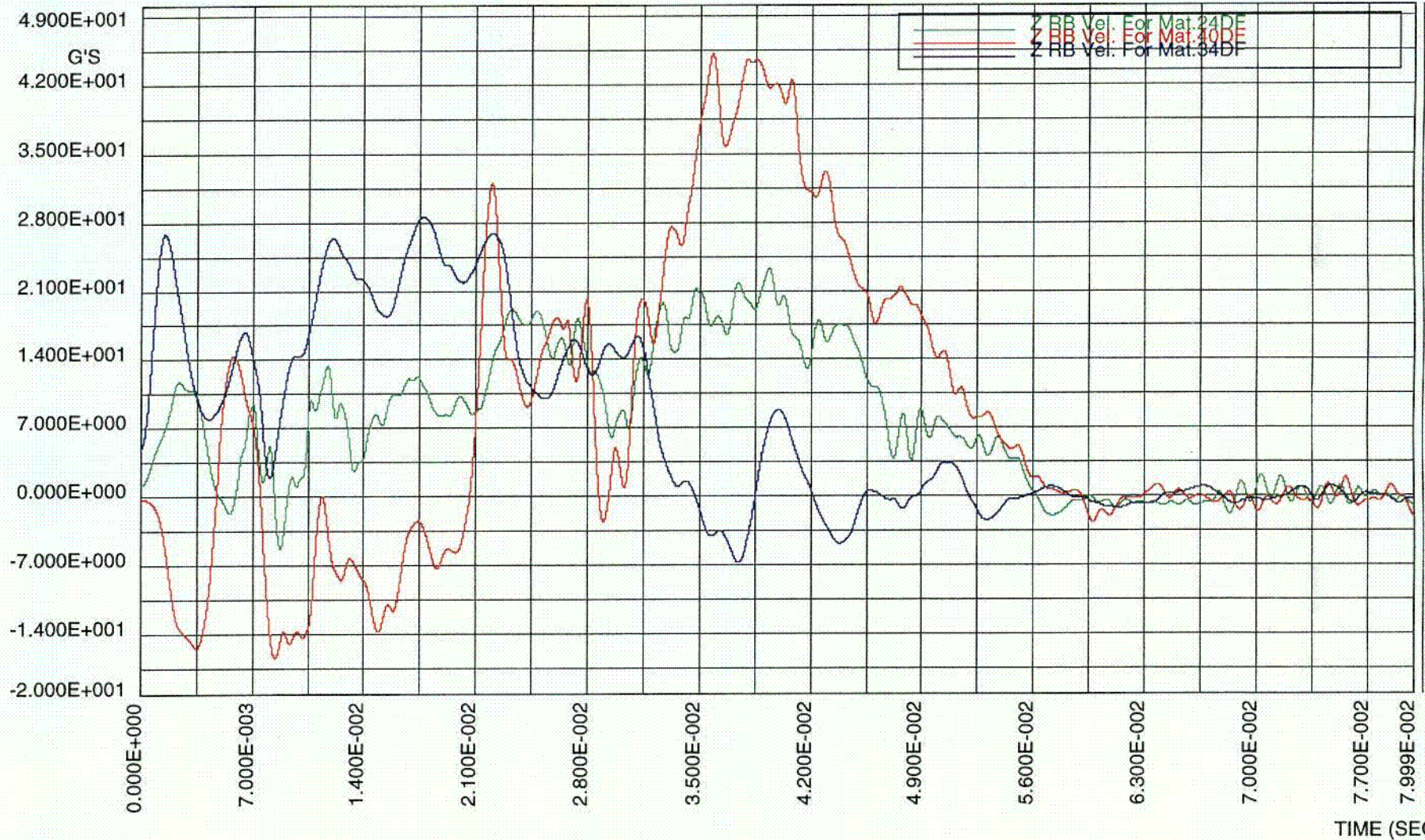
rcfor: 125 HI-TRACK V0=180.16 IN/SEC ESOIL=28 KSI

FIGURE 3.AN.16; FORCE AT MPC-TOP LID INTERFACE, SCENARIO B

HI-STORM FSAR  
 HI-2002444

Rev. 0

714



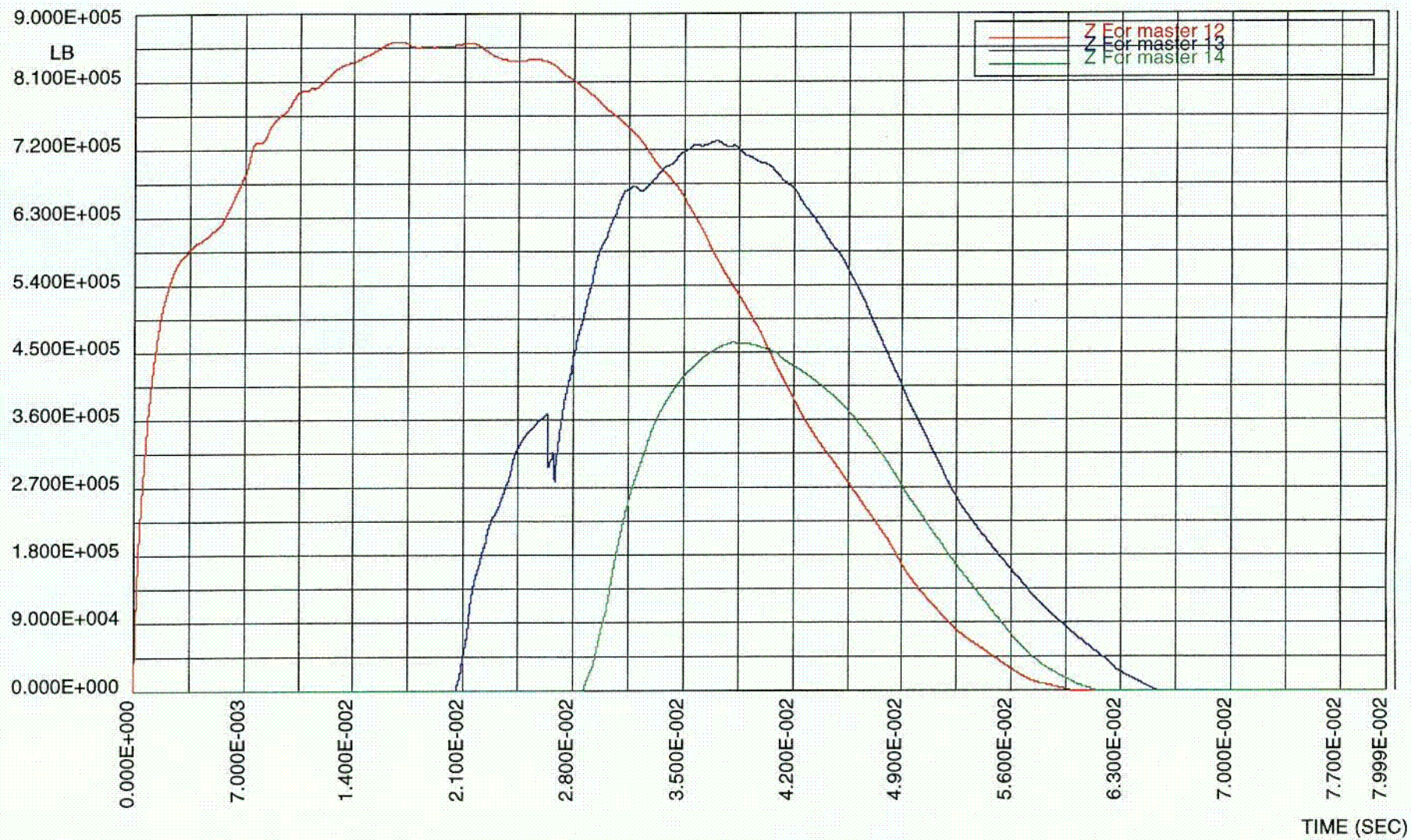
matsum: 100 HI-TRACK V0=180.16 IN/SEC ESOIL=28 KSI

FIGURE 3.AN.17; RIGID BODY DECELERATIONS TRANSFER LID, CENTROID, TOP LID, SCENARIO A

HI-STORM FSAR  
HI-2002444

C/S

Rev. 0



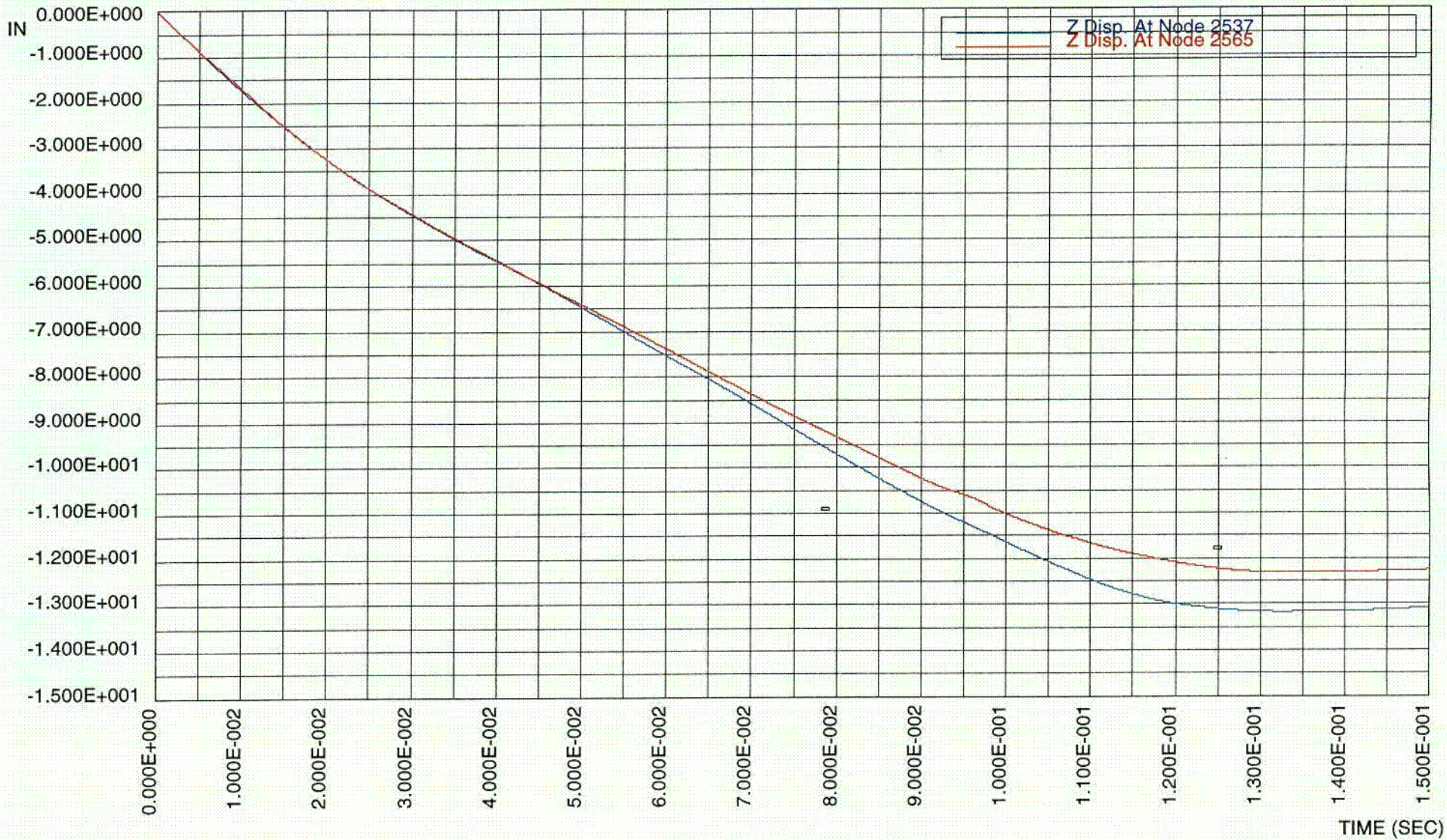
rcforc: 100 HI-TRACK V0=180.16 IN/SEC ESOIL=28 KSI

FIGURE 3.AN.18; INTERFACE FORCE AT TARGET (LOWER TRUNNION, WATER JACKET, UPPER TRUNNION)

HI-STORM FSAR  
 HI-2002444

910

Rev. 0



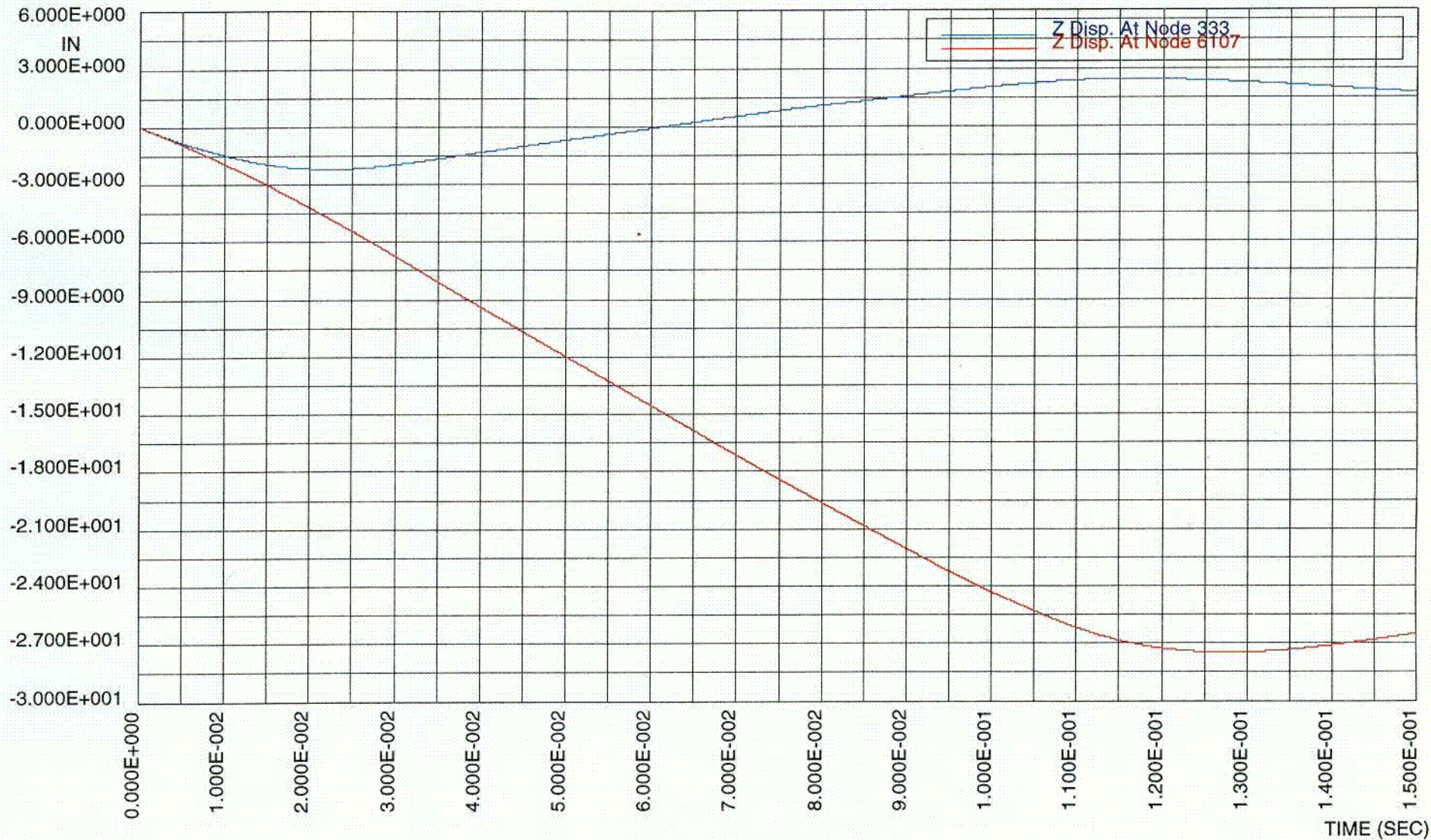
nodout: 125 HI-TRACK V0=180.16 IN/SEC ESOIL=28 KSI

FIGURE 3.AN.15; VERTICAL DISPLACEMENTS AT TOP AND BOTTOM OF INNER SHELL, SCENARIO B

HI-STORM FSAR  
HI-2002444

Rev. 0

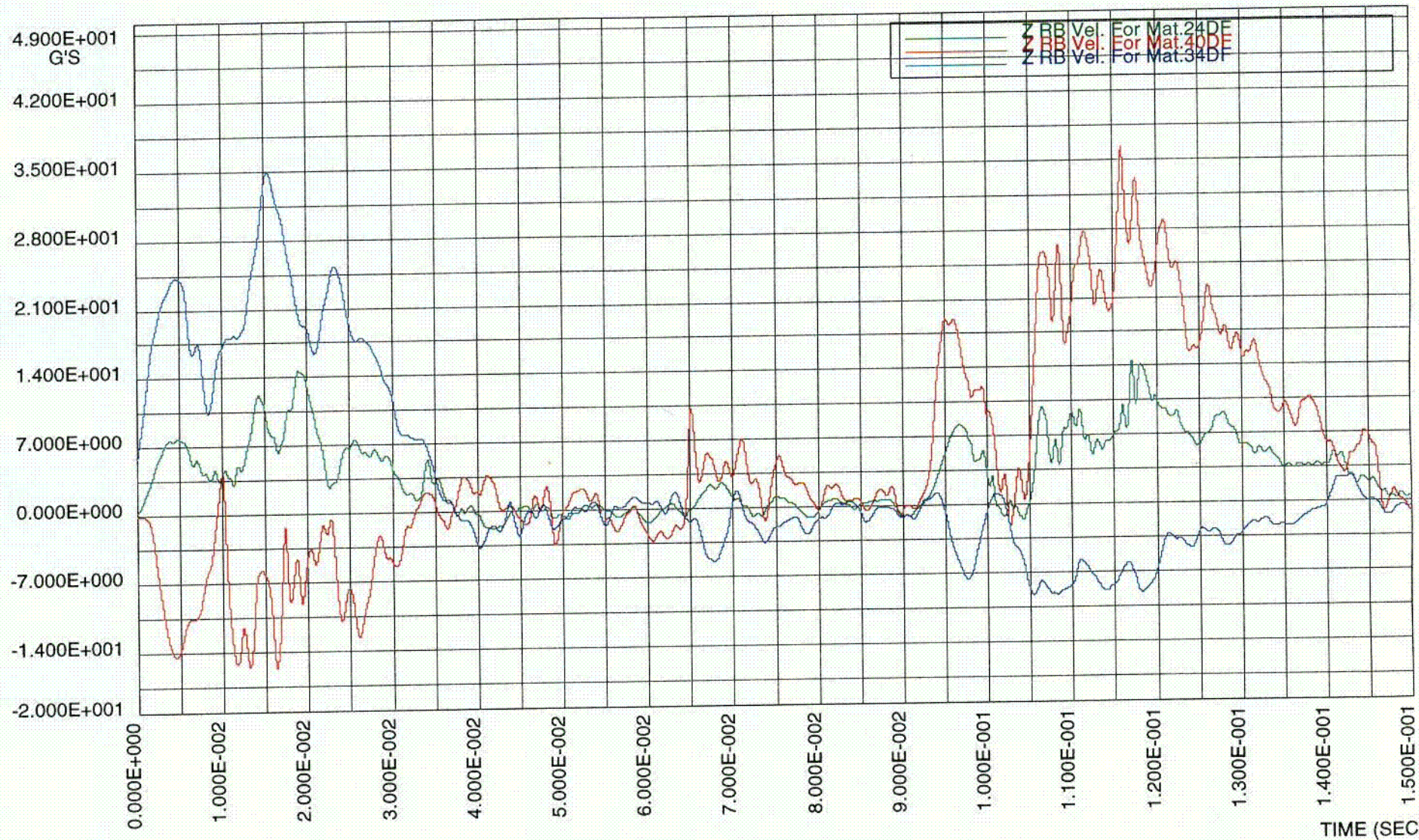
413



nodout: 100 HI-TRACK V0=180.16 IN/SEC ESOIL=28 KSI

HI-STORM FSAR HI-2002444 FIGURE 3.AN.20; VERTICAL DISPLACEMENT AT TRANSFER LID AND TOP LID, SCENARIO B

818



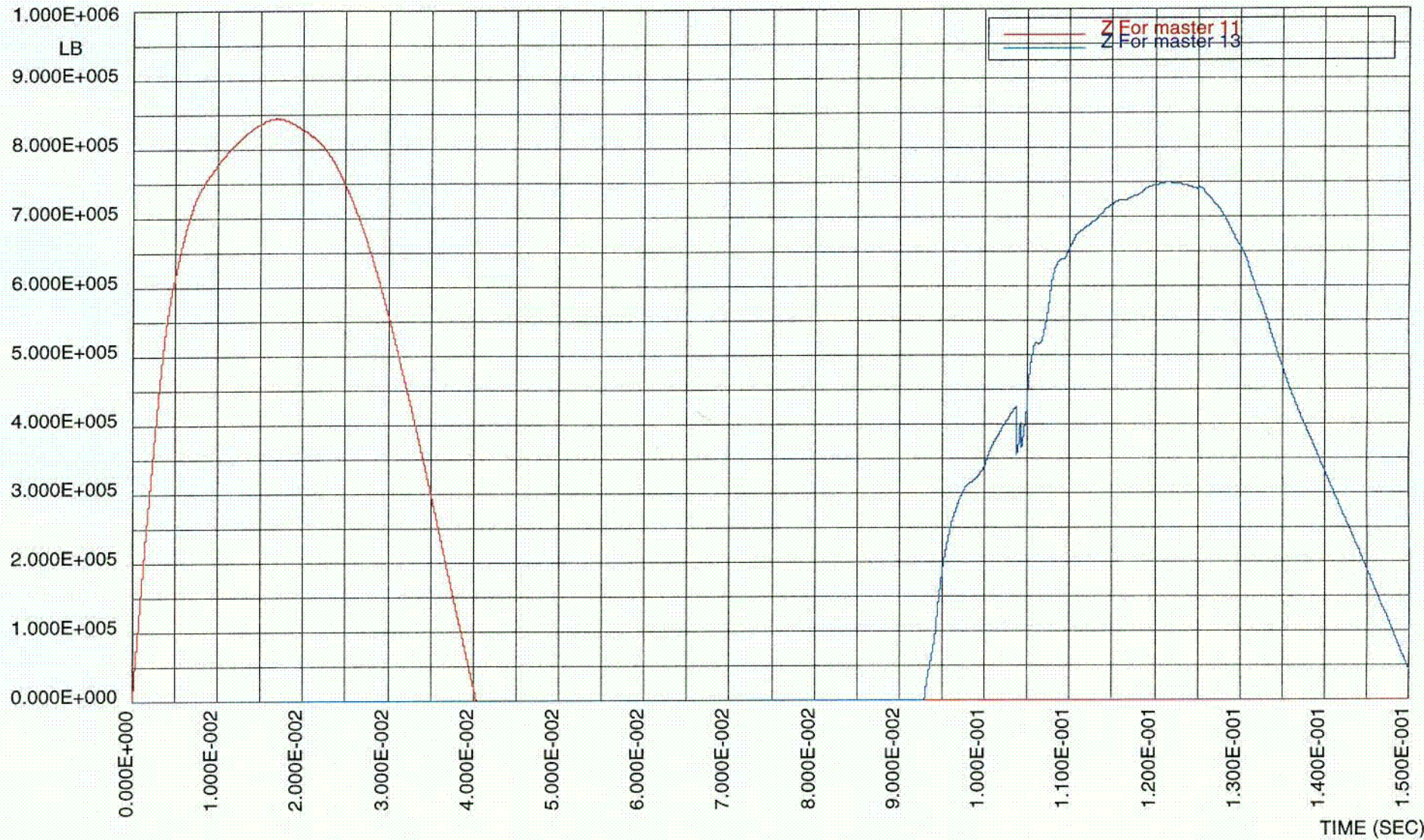
matsum: 100 HI-TRACK V0=180.16 IN/SEC ESOIL=28 KSI

FIGURE 3.AN.2I; RIGID BODY DECELERATIONS, SCENARIO B

HI-STORM FSAR  
HI-2002444

REV. 0

b19



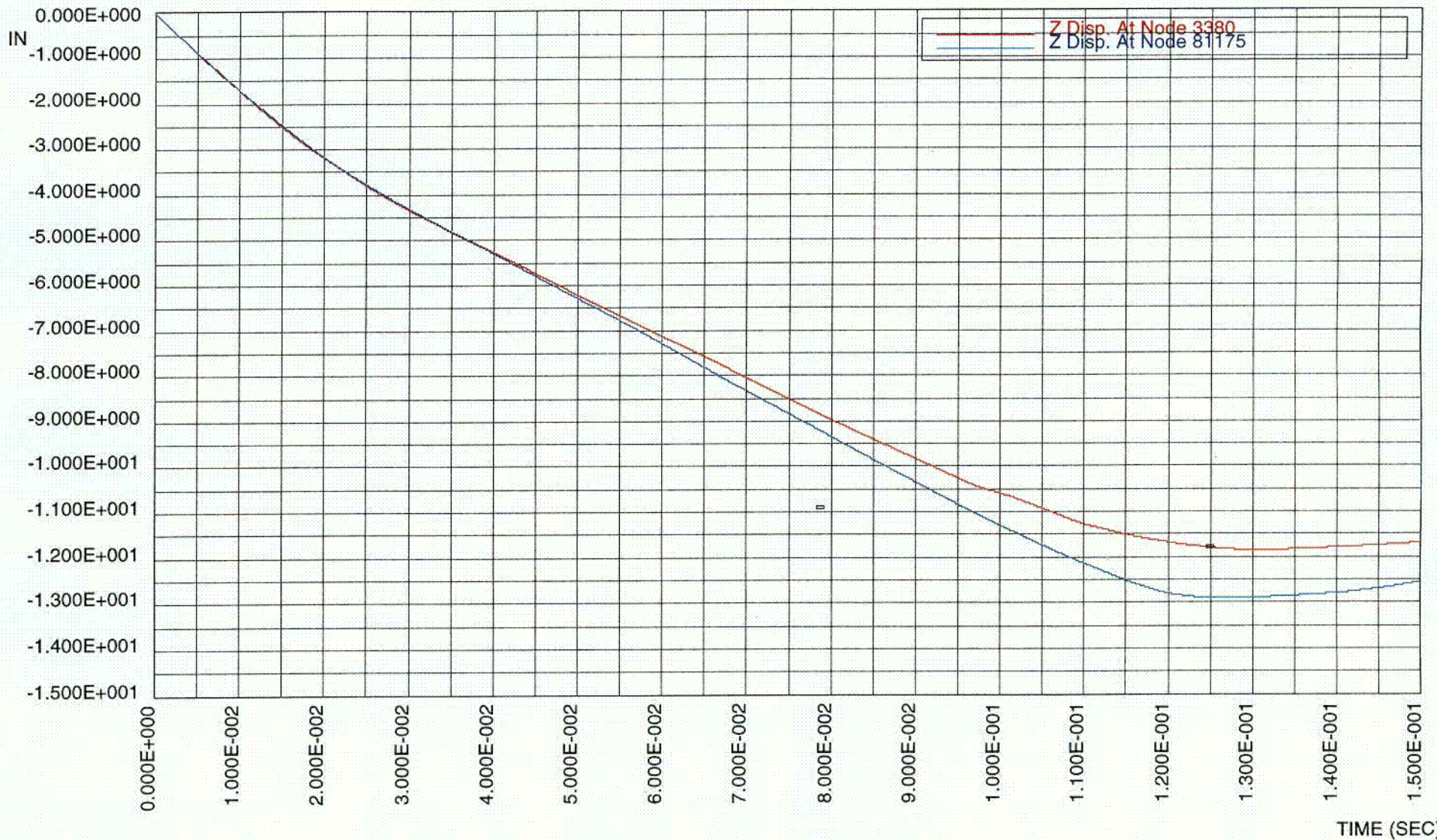
rcforc: 100 HI-TRACK V0=180.16 IN/SEC ESOIL=28 KSI

FIGURE 3.AN.22; FORCE AT TARGET IMPACT SITES, SCENARIO B

HI-STORM FSAR  
HI-2002444

C70

Rev. 0



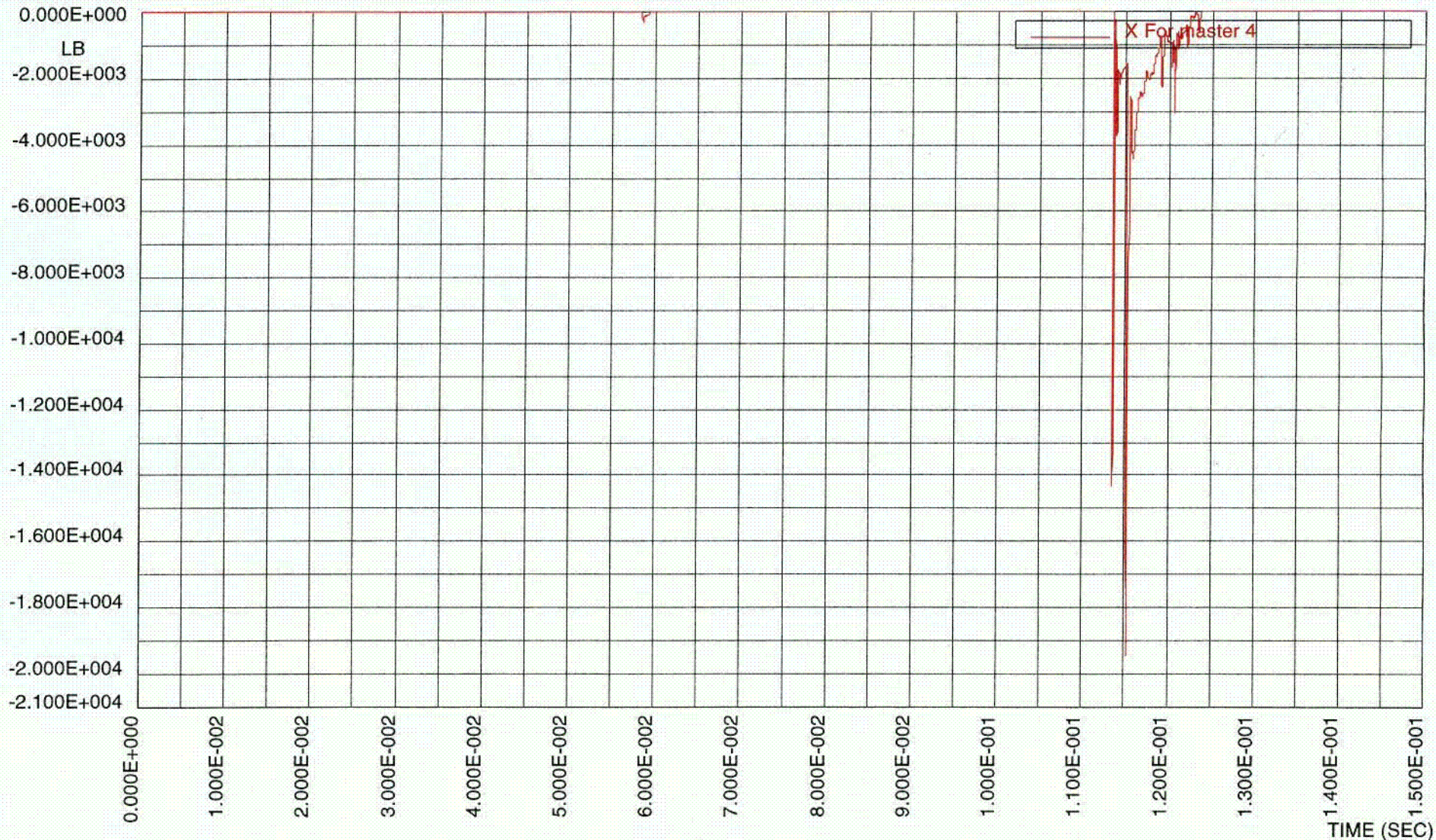
nodout: 100 HI-TRACK V0=180.16 IN/SEC ESOIL=28 KSI

FIGURE 3.AN.23; INNER SHELL VERTICAL DISPLACEMENTS—UPPER AND LOWER POINTS AT CENTROID

HI-STORM FSAR  
HI-2002444

REV. 0

C21



rforc: 100 HI-TRACK V0=180.16 IN/SEC ESOIL=28 KSI

HI-STORM FSAR  
HI-2002444

FIGURE 3.AN.24; INTERFACE FORCE-MPC/TOP LID IMPACT SITE, SCENARIO B

REV. 0

C122

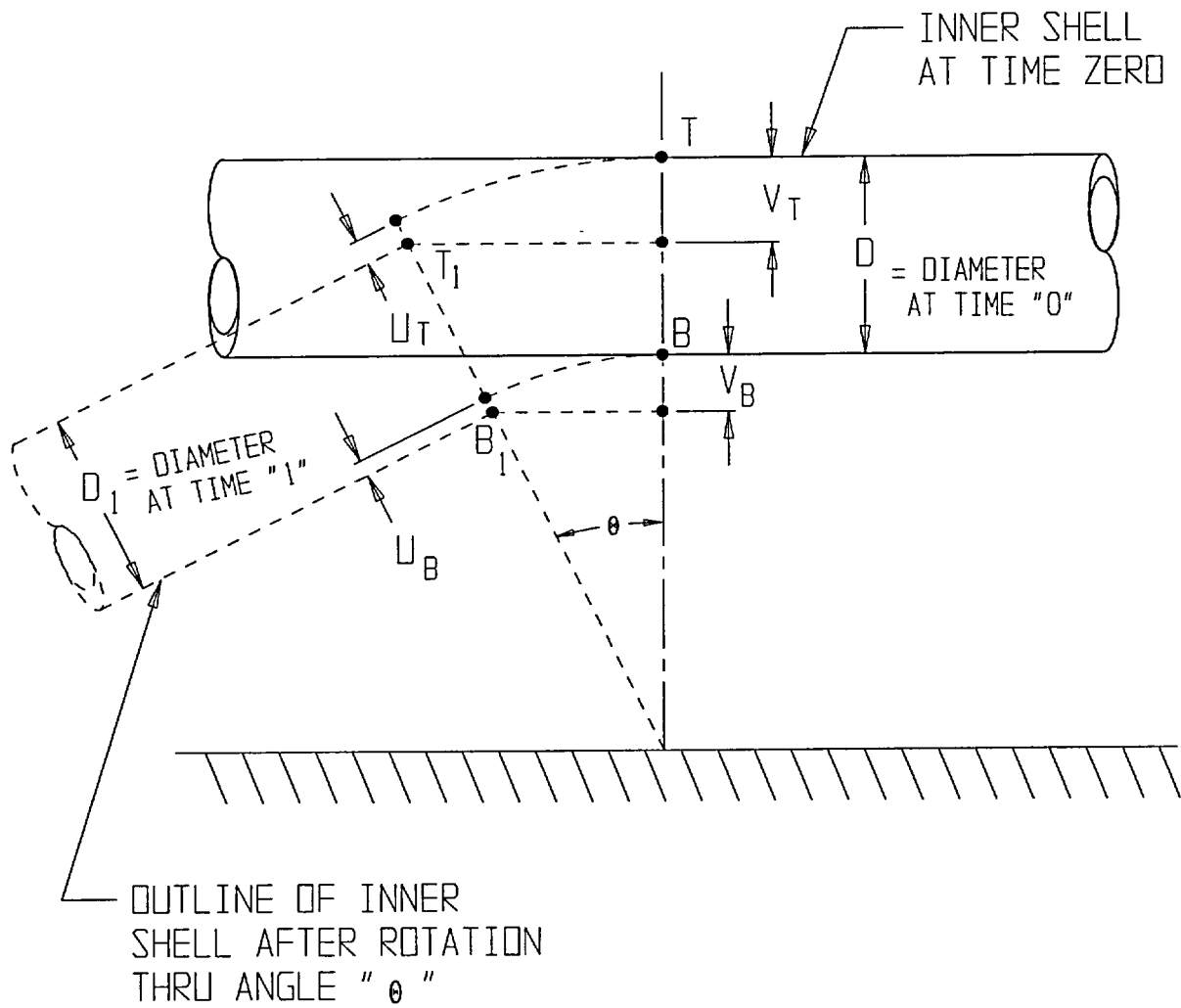
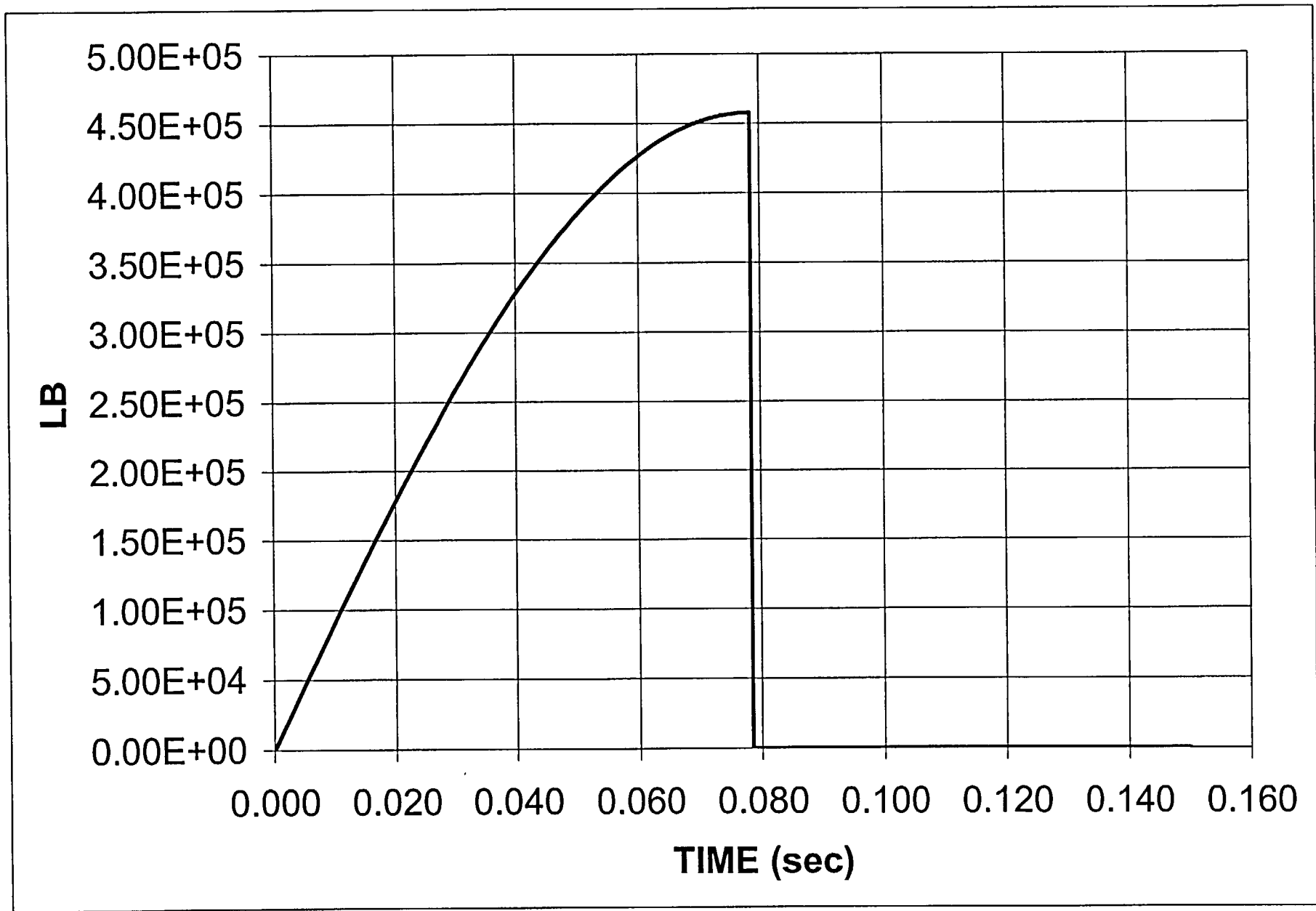


FIGURE 3.AN.25; GEOMETRY OF INNER SHELL DEFORMATION



125 HI-TRACK CAR IMPACT  
STEP 52 TIME = 7.7999242E-002  
MAX\_VONMISES

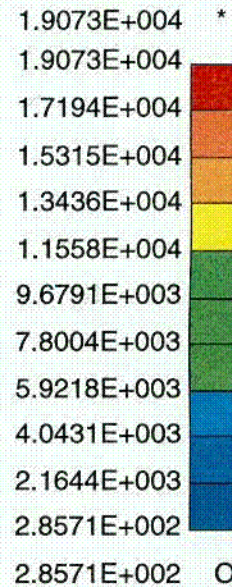
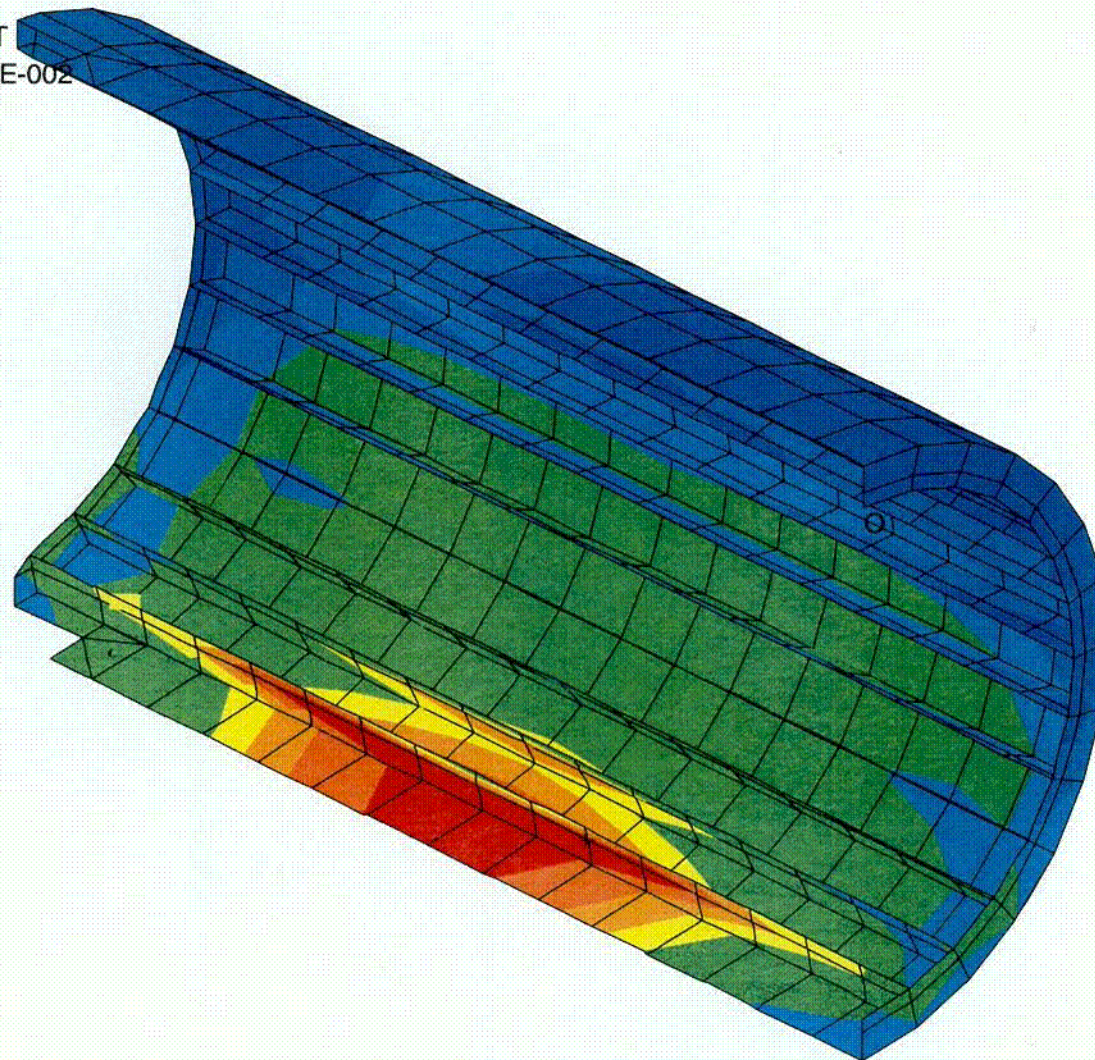
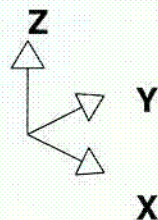


FIGURE 3.AN.27; VON MISES STRESS IN WATER JACKET-LARGE TORNADO MISSILE IMPACT ON 125 TON HI-TRAC

HI-STORM FSAR  
HI-2002444

C23

REV. 0

100 HI-TRACK CAR IMPACT  
STEP 52 TIME = 7.7999920E-002  
MAX\_VONMISES

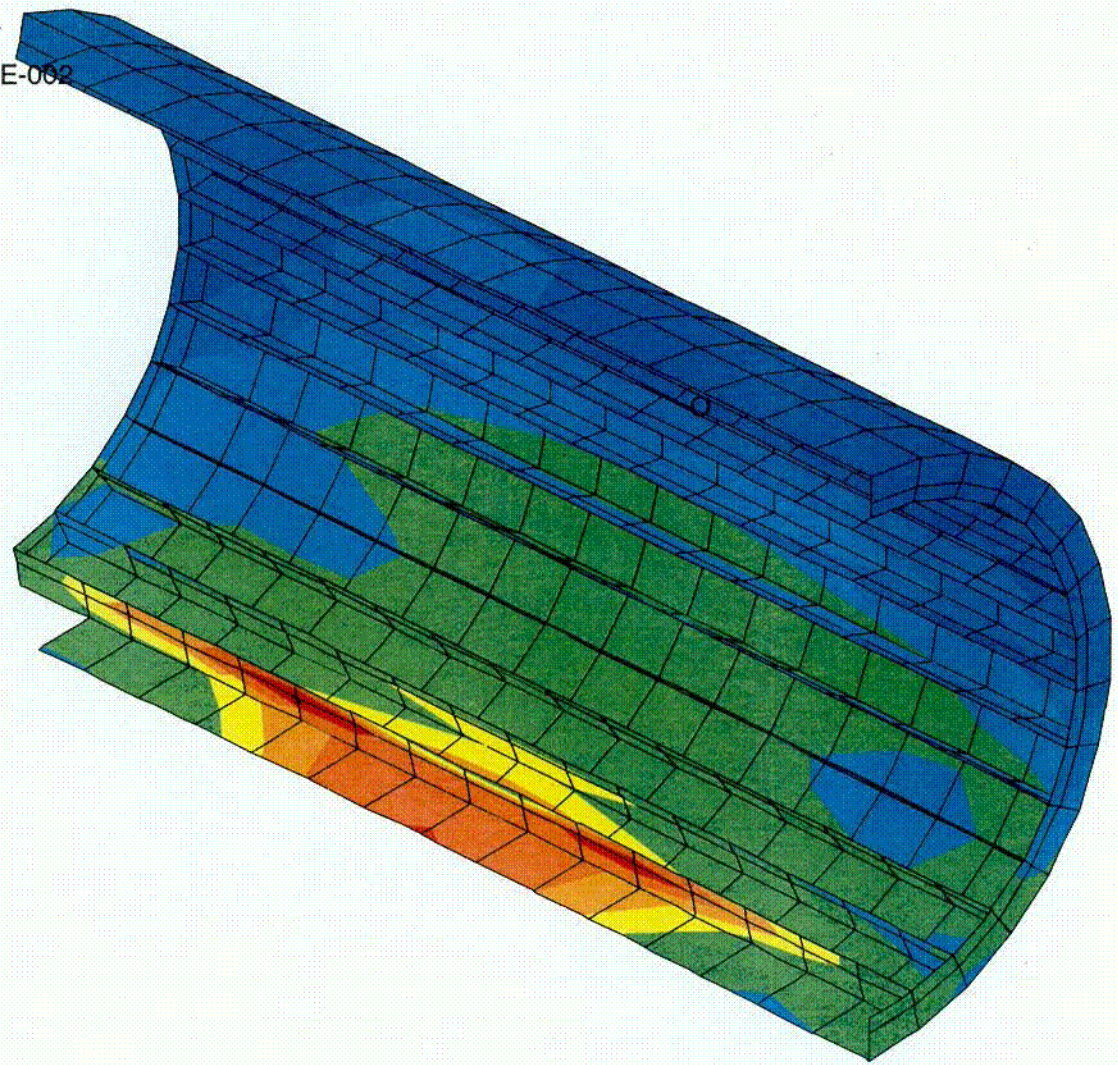
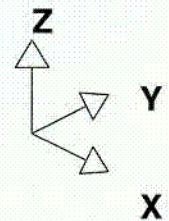
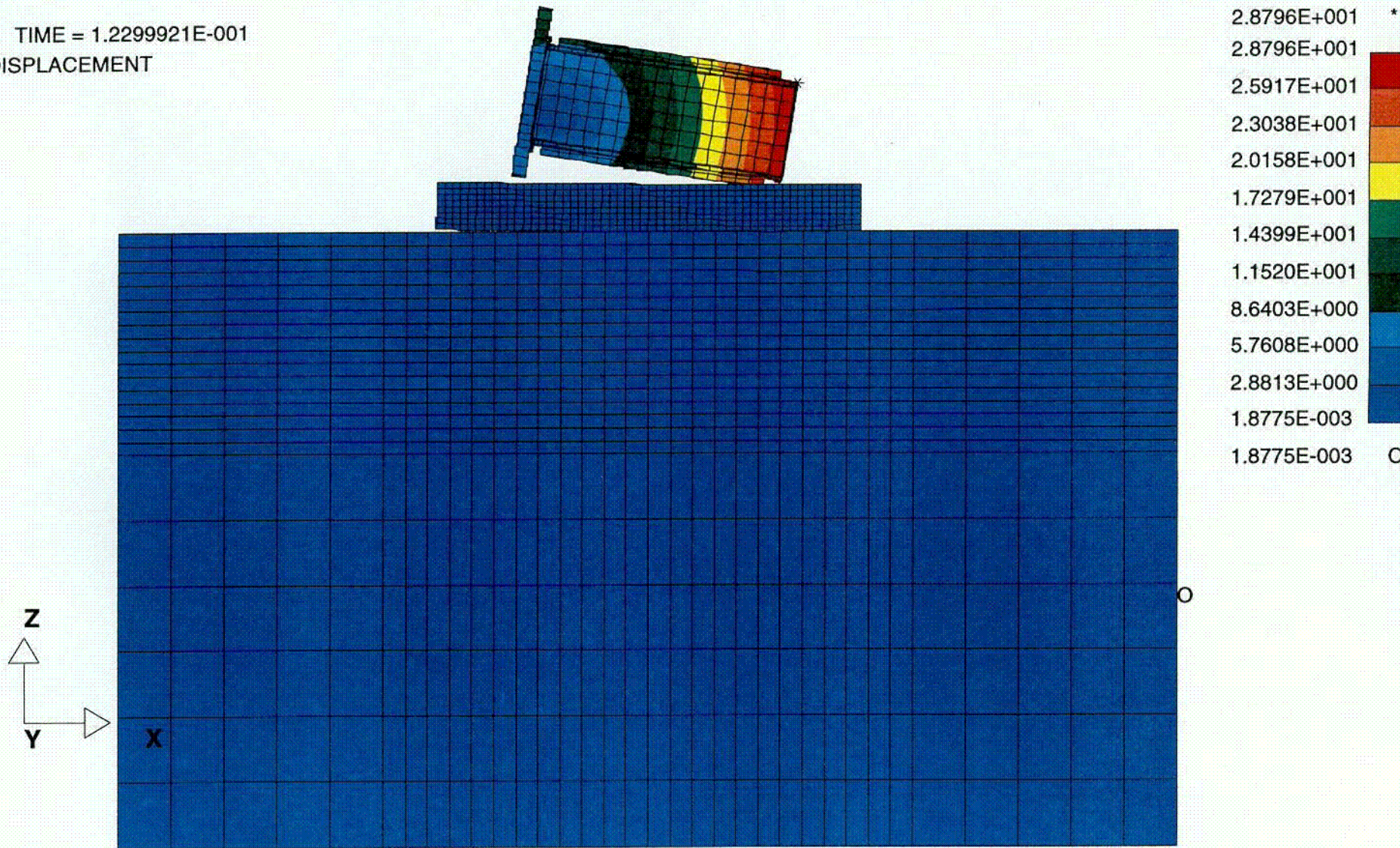


FIGURE 3.AN.28; VON MISES WATER JACKET-LARGE TORNADO MISSILE IMPACT ON 100 TON HI-TRAC

HI-STORM FSAR  
HI-2002444

C24

STEP 82 TIME = 1.2299921E-001  
TOTAL DISPLACEMENT

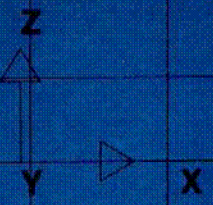
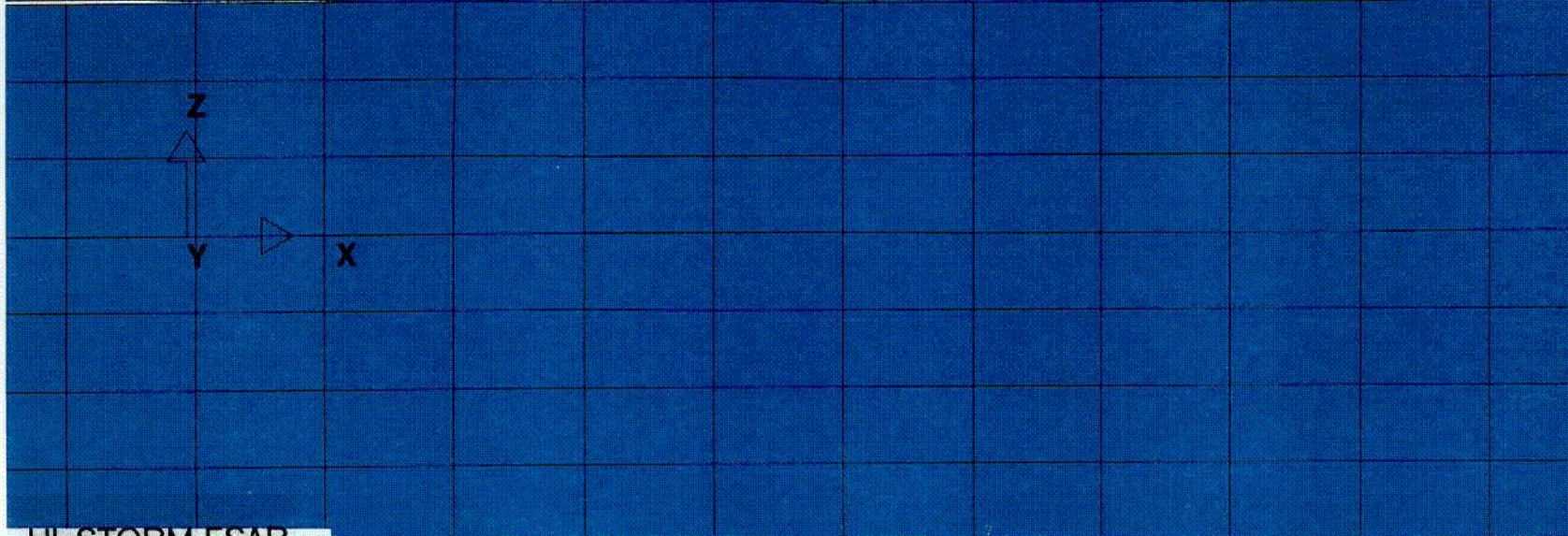
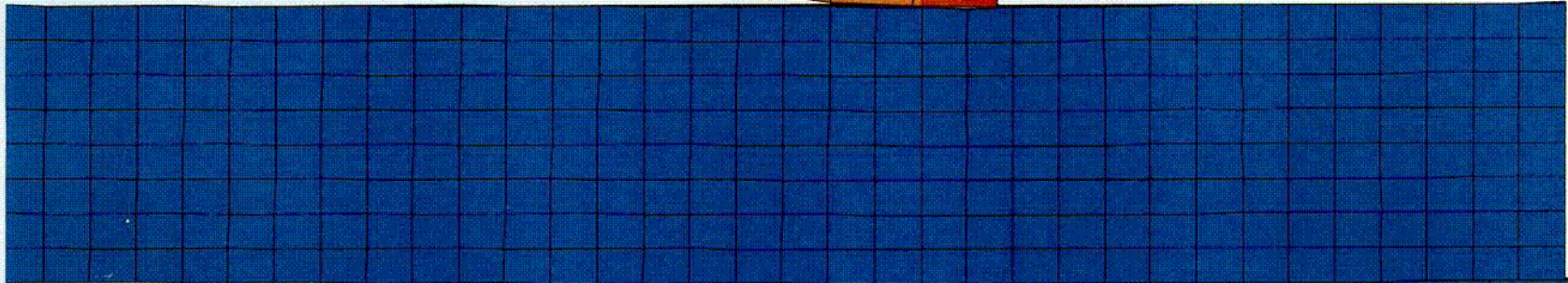
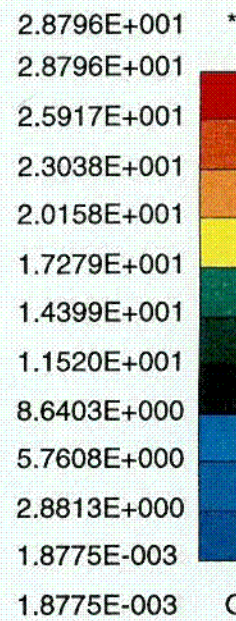
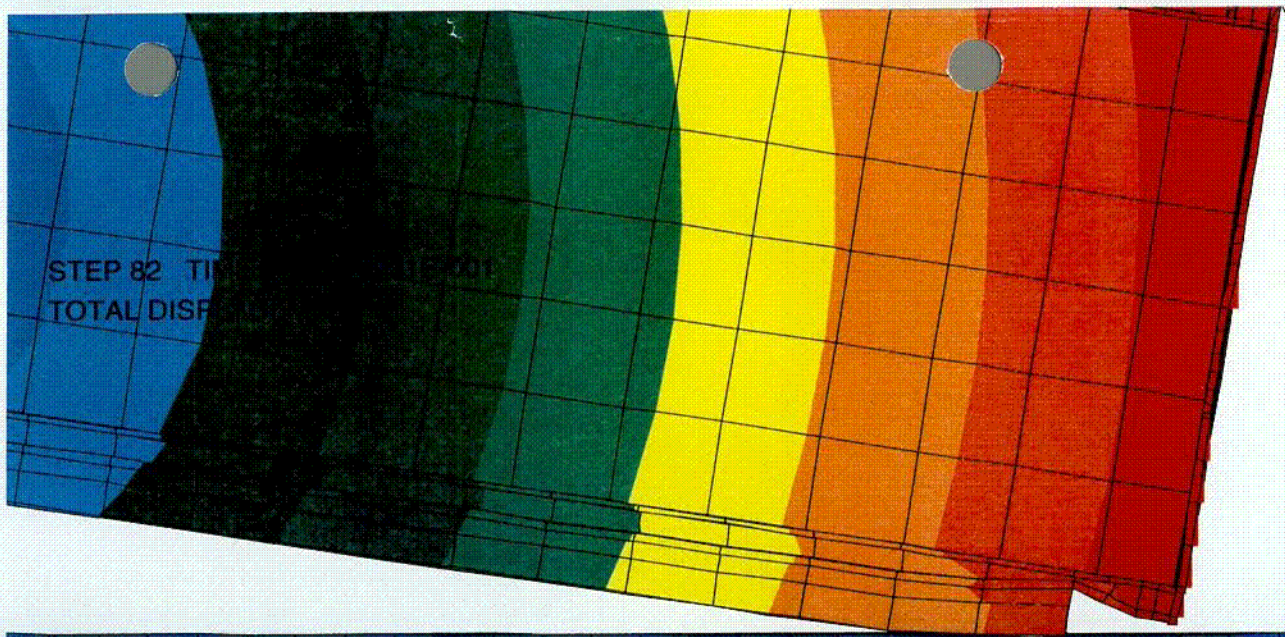


C25

HI-STORM FSAR  
HI-2002444

FIGURE 3.AN.29; SLAP DOWN OF HI-TRAC 100, SCENARIO B

REV. 0



C26

**Appendix 3.AO**

Not Used

|

**Appendix 3.AP**

Not Used

|

## APPENDIX 3.AQ: HI-STORM 100 COMPONENT THERMAL EXPANSIONS; MPC-24E

### 3.AQ.1 Scope

In this calculation, estimates of operating gaps, both radially and axially, are computed for the fuel basket-to-MPC shell, and for the MPC shell-to-overpack. This calculation is in support of the results presented in Section 3.4.4.2.

### 3.AQ.2 Methodology

Bounding temperatures are used to construct temperature distributions that will permit calculation of differential thermal expansions both radially and axially for the basket-to-MPC gaps, and for the MPC-to-overpack gaps. Reference temperatures are set at 70°F for all components. Temperature distributions are computed at the location of the HI-STORM 100 System where the temperatures are highest. A comprehensive nomenclature listing is provided in Section 3.AQ.6.

### 3.AQ.3 References

[3.AQ.1] Boley and Weiner, Theory of Thermal Stresses, John Wiley, 1960, Sec. 9.10, pp. 288-291.

[3.AQ.2] Burgreen, Elements of Thermal Stress Analysis, Arcturus Publishers, Cherry Hill NJ, 1988.

### 3.AQ.4 Calculations for Hot Components (Middle of System)

#### 3.AQ.4.1 Input Data

Based on thermal calculations in Chapter 4, the following temperatures are appropriate at the hottest axial location of the cask ( Table 4.4.27 and 4.4.36).

The temperature change at the overpack inner shell,  $\Delta T_{1h} := 199 - 70$

The temperature change at the overpack outer shell,  $\Delta T_{2h} := 145 - 70$

The temperature change at the mean radius of the MPC shell,  $\Delta T_{3h} := 347 - 70$

The temperature change at the outside of the MPC basket,  $\Delta T_{4h} := (492 - 70) \cdot 1.1$

The temperature change at the center of the basket (helium gas),  $\Delta T_{5h} := 650 - 70$

Note that the outer basket temperature is conservatively amplified by 10% to insure a bounding parabolic distribution. This conservatism serves to maximize the growth of the basket.

The geometry of the components are as follows:

The outer radius of the overpack,  $b := 66.25 \text{ in}$

The minimum inner radius of the overpack,  $a := 34.75 \text{ in}$

The mean radius of the MPC shell,  $R_{\text{mpc}} := \frac{68.375 \text{ in} - 0.5 \text{ in}}{2}$   $R_{\text{mpc}} = 33.938 \text{ in}$

The initial MPC-to-overpack radial clearance,  $RC_{\text{mo}} := 5 (69.5 - 68.5) \text{ in}$   
 $RC_{\text{mo}} = 0.5 \text{ in}$

This initial radial clearance value, used to perform a radial growth check, is conservatively based on the channel radius (see Dwg. 1495, Sh. 5) and the maximum MPC diameter. For axial growth calculations for the MPC-to-overpack lid clearance, the axial length of the overpack is defined as the distance from the top of the pedestal platform to the bottom of the lid bottom plate, and the axial length of the MPC is defined as the overall MPC height.

The axial length of the overpack,  $L_{\text{ovp}} := 191.5 \text{ in}$

The axial length of the MPC,  $L_{\text{mpc}} := 190.5 \text{ in}$

The initial MPC-to-overpack nominal axial clearance,  $AC_{\text{mo}} := L_{\text{ovp}} - L_{\text{mpc}}$

$$AC_{\text{mo}} = 1 \text{ in}$$

For growth calculations for the fuel basket-to-MPC shell clearances, the axial length of the basket is defined as the total length of the basket and the outer radius of the basket is defined as the mean radius of the MPC shell minus one-half of the shell thickness minus the initial basket-to-shell radial clearance.

The axial length of the basket,  $L_{\text{bas}} := 176.5 \text{ in}$

The initial basket-to-MPC lid nominal axial clearance,  $AC_{\text{bm}} := 1.8125 \text{ in}$

The initial basket-to-MPC shell nominal radial clearance,  $RC_{\text{bm}} := 0.1875 \text{ in}$

The outer radius of the basket,  $R_b := R_{\text{mpc}} - \frac{0.5}{2} \text{ in} - RC_{\text{bm}}$   $R_b = 33.5 \text{ in}$

The coefficients of thermal expansion used in the subsequent calculations are based on the mean temperatures of the MPC shell and the basket (conservatively estimated high).

The coefficient of thermal expansion for the MPC shell,  $\alpha_{\text{mpc}} := 9.015 \cdot 10^{-6}$

The coefficient of thermal expansion for the basket,  $\alpha_{\text{bas}} := 9.60 \cdot 10^{-6}$  600 deg. F

### 3.AQ.4.2 Thermal Growth of the Overpack

Results for thermal expansion deformation and stress in the overpack are obtained here. The system is replaced by a equivalent uniform hollow cylinder with approximated average properties.

Based on the given inside and outside surface temperatures, the temperature solution in the cylinder is given in the form:

$$C_a + C_b \cdot \ln\left(\frac{r}{a}\right)$$

where

$$C_a := \Delta T_{1h} \quad C_a = 129$$

$$C_b := \frac{\Delta T_{2h} - \Delta T_{1h}}{\ln\left(\frac{b}{a}\right)} \quad C_b = -83\,688$$

Next, form the integral relationship:

$$Int := \int_a^b \left[ C_a + C_b \cdot \ln\left(\frac{r}{a}\right) \right] \cdot r \, dr$$

The Mathcad program, which was used to create this appendix, is capable of evaluating the integral "Int" either numerically or symbolically. To demonstrate that the results are equivalent, the integral is evaluated both ways in order to qualify the accuracy of any additional integrations that are needed.

The result obtained through numerical integration,  $Int = 1.533 \times 10^5 \text{ in}^2$

To perform a symbolic evaluation of the solution the integral "Ints" is defined. This integral is then evaluated using the Maple symbolic math engine built into the Mathcad program as:

$$Int_s := \int_a^b \left[ C_a + C_b \cdot \ln\left(\frac{r}{a}\right) \right] \cdot r \, dr$$

$$Int_s := \frac{1}{2} \cdot C_b \cdot \ln\left(\frac{b}{a}\right) \cdot b^2 + \frac{1}{2} \cdot C_a \cdot b^2 - \frac{1}{4} \cdot C_b \cdot b^2 + \frac{1}{4} \cdot C_b \cdot a^2 - \frac{1}{2} \cdot C_a \cdot a^2$$

$$Int_s = 1.533 \times 10^5 \text{ in}^2$$

We note that the values of  $\text{Int}$  and  $\text{Int}_s$  are identical. The average temperature in the overpack cylinder ( $T_{\text{bar}}$ ) is therefore determined as:

$$T_{\text{bar}} = \frac{2}{(b^2 - a^2)} \cdot \text{Int} \quad T_{\text{bar}} = 96.348$$

We estimate the average coefficient of thermal expansion for the overpack by weighting the volume of the various layers. A total of four layers are identified for this calculation. They are:

- 1) the inner shell
- 2) the shield shell
- 3) the radial shield
- 4) the outer shell

Note that the shield shell was removed from the HI-STORM 100 design as of 6.01. The replacement of the shield shell with concrete, however, has a negligible effect on the resultant coefficient of thermal expansion because (a) the difference in thermal expansion coefficients between concrete and carbon steel is small and (b) the shield shell accounts for a small percentage of the total overpack radial thickness.

Thermal properties are based on estimated temperatures in the component and coefficient of thermal expansion values taken from the tables in Chapter 3. The following averaging calculation involves the thicknesses ( $t$ ) of the various components, and the estimated coefficients of thermal expansion at the components' mean radial positions. The results of the weighted average process yields an effective coefficient of linear thermal expansion for use in computing radial growth of a solid cylinder (the overpack).

The thicknesses of each component are defined as:

$$t_1 = 1.25 \text{ m} \quad t_2 = 0.75 \text{ m} \quad t_3 = 26.75 \text{ in} \quad t_4 = 0.75 \text{ m}$$

and the corresponding mean radii can therefore be defined as:

$$r_1 := a + .5 t_1 + 2.0 \text{ m} \quad (\text{add the channel depth})$$

$$r_2 := r_1 + .5 t_1 + .5 t_2$$

$$r_3 := r_2 + .5 t_2 + .5 t_3$$

$$r_4 := r_3 + .5 t_3 + .5 t_4$$

To check the accuracy of these calculations, the outer radius of the overpack is calculated from  $r_4$  and  $t_4$ , and the result is compared with the previously defined value (b).

$$b_1 := r_4 + 0.5 \cdot t_4$$

$$b_1 = 66.25 \text{ in}$$

$$b = 66.25 \text{ in}$$

We note that the calculated value  $b_1$  is identical to the previously defined value  $b$ . The coefficients of thermal expansion for each component, estimated based on the temperature gradient, are defined as:

$$\alpha_1 := 5.782 \cdot 10^{-6}$$

$$\alpha_2 := 5.782 \cdot 10^{-6}$$

$$\alpha_3 := 5.5 \cdot 10^{-6}$$

$$\alpha_4 := 5.638 \cdot 10^{-6}$$

Thus, the average coefficient of thermal expansion of the overpack is determined as:

$$\alpha_{avg} := \frac{r_1 \cdot t_1 \cdot \alpha_1 + r_2 \cdot t_2 \cdot \alpha_2 + r_3 \cdot t_3 \cdot \alpha_3 + r_4 \cdot t_4 \cdot \alpha_4}{\frac{a+b}{2} \cdot (t_1 + t_2 + t_3 + t_4)}$$
$$\alpha_{avg} = 5.628 \times 10^{-6}$$

Reference 3.AQ.1 gives an expression for the radial deformation due to thermal growth. At the inner radius of the overpack ( $r = a$ ), the radial growth is determined as:

$$\Delta R_{ah} := \alpha_{avg} \cdot a \cdot T_{bar}$$

$$\Delta R_{ah} = 0.019 \text{ in}$$

Similarly, an overestimate of the axial growth of the overpack can be determined by applying the average temperature ( $T_{bar}$ ) over the entire length of the overpack as:

$$\Delta L_{ovph} := L_{ovp} \cdot \alpha_{avg} \cdot T_{bar}$$

$$\Delta L_{ovph} = 0.104 \text{ in}$$

Estimates of the secondary thermal stresses that develop in the overpack due to the radial temperature variation are determined using a conservatively high value of  $E$  as based on the temperature of the steel. The circumferential stress at the inner and outer surfaces ( $\sigma_{ca}$  and  $\sigma_{cb}$ , respectively) are determined as:

The Young's Modulus of the material,  $E := 28300000 \cdot \text{psi}$

$$\sigma_{ca} := \alpha_{avg} \cdot \frac{E}{a^2} \left[ 2 \frac{a^2}{(b^2 - a^2)} \text{Int} - (C_a) a^2 \right]$$

$$\sigma_{ca} = -5200 \text{ psi}$$

$$\sigma_{cb} := \alpha_{avg} \cdot \frac{E}{b^2} \left[ 2 \frac{b^2}{(b^2 - a^2)} \cdot \text{Int} - \left[ C_a + C_b \cdot \left( \ln \left( \frac{b}{a} \right) \right) \right] \cdot b^2 \right]$$

$$\sigma_{cb} = 3400 \text{ psi}$$

The radial stress due to the temperature gradient is zero at both the inner and outer surfaces of the overpack. The radius where a maximum radial stress is expected, and the corresponding radial stress, are determined by trial and error as:

$$N := 0.37$$

$$r := a(1 - N) + N \cdot b$$

$$r = 46.405 \text{ in}$$

$$\sigma_r := \alpha_{avg} \frac{E}{r^2} \left[ \frac{r^2 - a^2}{2} \cdot T_{bar} - \int_a^r \left[ C_a + C_b \left( \ln \left( \frac{y}{a} \right) \right) \right] \cdot y \, dy \right]$$

$$\sigma_r = -678.201 \text{ psi}$$

The axial stress developed due to the temperature gradient is equal to the sum of the radial and tangential stresses at any radial location. (see eq. 9.10.7) of [3.AQ.1]. Therefore, the axial stresses are available from the above calculations. The stress intensities in the overpack due to the temperature distribution are below the Level A membrane stress.

### 3 AQ.4.3 Thermal Growth of the MPC Shell

The radial and axial growth of the MPC shell ( $\Delta R_{mpch}$  and  $\Delta L_{mpch}$ , respectively) are determined as:

$$\Delta R_{mpch} := \alpha_{mpc} \cdot R_{mpc} \cdot \Delta T_{3h} \quad \Delta R_{mpch} = 0.085 \text{ in}$$

$$\Delta L_{mpch} := \alpha_{mpc} \cdot L_{mpc} \cdot \Delta T_{3h} \quad \Delta L_{mpch} = 0.476 \text{ in}$$

### 3.AQ.4.4 Clearances Between the MPC Shell and Overpack

The final radial and axial MPC shell-to-overpack clearances ( $RG_{moh}$  and  $AG_{moh}$ , respectively) are determined as:

$$RG_{moh} := RC_{mo} + \Delta R_{ah} - \Delta R_{mpch}$$

$$RG_{moh} = 0.434 \text{ in}$$

$$AG_{moh} := AC_{mo} + \Delta L_{ovph} - \Delta L_{mpch}$$

$$AG_{moh} = 0.628 \text{ in}$$

Note that this axial clearance ( $AG_{moh}$ ) is based on the temperature distribution at the hottest axial location in the system.

### 3.AQ.4.5 Thermal Growth of the MPC-24E Basket

Using formulas given in [3.AQ.2] for a solid body of revolution, and assuming a parabolic temperature distribution in the radial direction with the center and outer temperatures given previously, the following relationships can be developed for free thermal growth.

$$\text{Define } \Delta T_{bas} := \Delta T_{5h} - \Delta T_{4h} \quad \Delta T_{bas} = 115.8$$

$$\text{Then the mean temperature can be defined as } T_{bar} := \frac{2}{R_b^2} \int_0^{R_b} \left( \Delta T_{5h} - \Delta T_{bas} \cdot \frac{r^2}{R_b^2} \right) \cdot r \, dr$$

Using the Maple symbolic engine again, the closed form solution of the integral is:

$$T_{bar} := \frac{2}{R_b^2} \cdot \left( \frac{-1}{4} \cdot \Delta T_{bas} \cdot R_b^2 + \frac{1}{2} \cdot \Delta T_{5h} \cdot R_b^2 \right)$$

$$T_{bar} = 522.1$$

The corresponding radial growth at the periphery ( $\Delta R_{bh}$ ) is therefore determined as:

$$\Delta R_{bh} := \alpha_{bas} \cdot R_b \cdot T_{bar} \quad \Delta R_{bh} = 0.168 \text{ in}$$

and the corresponding axial growth ( $\Delta L_{bas}$ ) is determined from [3.AQ.2] as:

$$\Delta L_{bh} := \Delta R_{bh} \cdot \frac{L_{bas}}{R_b}$$

$$\Delta L_{bh} = 0.885 \text{ in}$$

Note that the coefficient of thermal expansion for the hottest basket temperature has been used, and the results are therefore conservative.

### 3.AQ.4.6 Clearances Between the Fuel Basket and MPC Shell

The final radial and axial fuel basket-to-MPC shell and lid clearances ( $RG_{bmh}$  and  $AG_{bmh}$ , respectively) are determined as:

$$RG_{bmh} := RC_{bm} - \Delta R_{bh} + \Delta R_{mpch}$$

$$RG_{bmh} = 0.104 \text{ in}$$

$$AG_{bmh} := AC_{bm} - \Delta L_{bh} + \Delta L_{mpch}$$

$$AG_{bmh} = 1.404 \text{ in}$$

### 3 AQ 5 Summary of Results

The previous results are summarized here

MPC Shell-to-Overpack

Fuel Basket-to-MPC Shell

$$RG_{moh} = 0.434 \text{ in}$$

$$RG_{bmh} = 0.104 \text{ in}$$

$$AG_{moh} = 0.628 \text{ in}$$

$$AG_{bmh} = 1.404 \text{ in}$$

### 3.AQ.6 Nomenclature

$a$  is the inner radius of the overpack

$AC_{bm}$  is the initial fuel basket-to-MPC axial clearance.

$AC_{mo}$  is the initial MPC-to-overpack axial clearance.

$AG_{bmh}$  is the final fuel basket-to-MPC shell axial gap for the hot components.

$AG_{moh}$  is the final MPC shell-to-overpack axial gap for the hot components.

$b$  is the outer radius of the overpack.

$L_{bas}$  is the axial length of the fuel basket.

$L_{mpc}$  is the axial length of the MPC.

$L_{ovp}$  is the axial length of the overpack.

$r_1$  ( $r_2, r_3, r_4$ ) is mean radius of the overpack inner shell (shield shell, concrete, outer shell).

$R_b$  is the outer radius of the fuel basket.

$R_{mpc}$  is the mean radius of the MPC shell.

$RC_{bm}$  is the initial fuel basket-to-MPC radial clearance.

$RC_{mo}$  is the initial MPC shell-to-overpack radial clearance.

$RG_{bmh}$  is the final fuel basket-to-MPC shell radial gap for the hot components.

$RG_{moh}$  is the final MPC shell-to-overpack radial gap for the hot components.

$t_1$  ( $t_2, t_3, t_4$ ) is the thickness of the overpack inner shell (shield shell, concrete, outer shell).

$T_{bar}$  is the average temperature of the overpack cylinder.

$\alpha_1$  ( $\alpha_2, \alpha_3, \alpha_4$ ) is the coefficient of thermal expansion of the overpack inner shell (shield shell, concrete, outer shell).

$\alpha_{avg}$  is the average coefficient of thermal expansion of the overpack.

$\alpha_{bas}$  is the coefficient of thermal expansion of the overpack.

$\alpha_{mpc}$  is the coefficient of thermal expansion of the MPC.

$\Delta L_{bh}$  is the axial growth of the fuel basket for the hot components.

$\Delta L_{mpch}$  is the axial growth of the MPC for the hot components.  
 $\Delta L_{ovph}$  is the axial growth of the overpack for the hot components.  
 $\Delta R_{ah}$  is the radial growth of the overpack inner radius for the hot components.  
 $\Delta R_{bh}$  is the radial growth of the fuel basket for the hot components.  
 $\Delta R_{mpch}$  is the radial growth of the MPC shell for the hot components.  
 $\Delta T_{1h}$  is the temperature change at the overpack inner shell for hot components.  
 $\Delta T_{2h}$  is the temperature change at the overpack outer shell for hot components.  
 $\Delta T_{3h}$  is the temperature change at the MPC shell mean radius for hot components.  
 $\Delta T_{4h}$  is the temperature change at the MPC basket periphery for hot components.  
 $\Delta T_{5h}$  is the temperature change at the MPC basket centerline for hot components.  
 $\Delta T_{bas}$  is the fuel basket centerline-to-periphery temperature gradient.  
 $\sigma_{ca}$  is the circumferential stress at the overpack inner surface.  
 $\sigma_{cb}$  is the circumferential stress at the overpack outer surface.  
 $\sigma_r$  is the maximum radial stress of the overpack  
 $\sigma_{z1}$  is the axial stress at the fuel basket centerline.  
 $\sigma_{z0}$  is the axial stress at the fuel basket periphery.

## APPENDIX 3.AR - ANALYSIS OF TRANSNUCLEAR DAMAGED FUEL CANISTER AND THORIA ROD CANISTER

### 3.AR.1 Introduction

Some of the items at the Dresden Station that have been considered for storage in the HI-STAR 100 System are damaged fuel stored in Transnuclear damaged fuel canisters and Thoria rods that are also stored in a special canister designed by Transnuclear. Both of these canisters have been designed and have been used by ComEd to transport the damaged fuel and the Thoria rods. Despite the previous usage of these canisters, it is prudent and appropriate to provide an independent structural analysis of the major load path of these canisters prior to accepting them for inclusion as permitted items in the HI-STAR and HI-STORM 100 MPC's. This appendix contains the necessary structural analysis of the Transnuclear damaged fuel canister and Thoria rod canister. The objective of the analysis is to demonstrate that the canisters are structurally adequate to support the loads that develop during normal lifting operations and during postulated accident conditions.

The upper closure assembly is designed to meet the requirements of NUREG-0612 [2]. The remaining components of the canisters are governed by ASME Code Section III, Subsection NG [3]. These are the same criteria used in Appendix 3.B of the HI-STAR 100 to analyze the Holtec damaged fuel container for Dresden damaged fuel.

### 3.AR.2 Composition

This appendix was created using the Mathcad (version 8.02) software package. Mathcad uses the symbol ':=' as an assignment operator, and the equals symbol '=' retrieves values for constants or variables.

### 3.AR.3 References

1. Crane Manufacture's of America Association, Specifications for Electric Overhead Traveling Cranes #70.
2. NUREG-0612, Control of Heavy Loads at Nuclear Power Plants
3. ASME Boiler and Pressure Vessel Code, Section III, July 1995

### 3.AR.4 Assumptions

1. Buckling is not a concern during an accident since during a drop the canister will be confined by the fuel basket.
2. The strength of the weld is assumed to decrease the same as the base metal as the temperature increases.

### 3.AR.5 Method

Two are considered: 1) normal lifting and handling of canister, and 2) accident drop event.

### 3.AR.6 Acceptance Criteria

#### 1) Normal Handling -

a) Canister governed by ASME NG allowables:

b) Welds governed by NG and NF allowables;  
quality factors taken from NG  
stress limit = 0.3 Su

c) Lifting governed by NUREG-0612 allowables.

#### 2) Drop Accident -

a) canister governed by ASME NG allowables:  
shear = 0.42 Su (conservative)

b) Welds governed by NG and NF allowables;  
quality factors taken from NG  
stress limit = 0.42 Su

### 3.AR.7 Input Stress Data

The canisters is handled while still in the spent fuel pool. Therefore, its design temperature for lifting considerations is the temperature of the fuel pool water (150°F). The design temperature for accident conditions is 725°F. All dimensions are taken from the Transnuclear design drawings listed at the end of this appendix. The basic input parameters used to perform the calculations are:

Design stress intensity of SA240-304 (150°F)	$S_{m1} := 20000 \text{ psi}$
Design stress intensity of SA240-304 (775°F)	$S_{m2} := 15800 \text{ psi}$
Yield stress of SA240-304 (150°F)	$S_{y1} := 27500 \text{ psi}$
Yield stress of SA240-304 (775°F)	$S_{y2} := 17500 \text{ psi}$
Ultimate strength of SA240-304 (150°F)	$S_{u1} := 73000 \text{ psi}$
Ultimate strength of SA240-304 (775°F)	$S_{u2} := 63300 \text{ psi}$

Ultimate strength of weld material (150°F)	$S_{u_w} := 70000 \text{ psi}$
Ultimate strength of weld material (775°F)	$S_{u_{wacc}} := S_{u_w} - (S_{u1} - S_{u2})$
Weight of a BWR fuel assembly (D-1)	$W_{fuel} := 400 \text{ lbf}$
Weight of 18 Thoria Rods (Calculated by Holtec)	$W_{thoria} := 90 \text{ lbf}$
Bounding Weight of the damaged fuel canister (Estimated by Holtec)	$W_{container} := 150 \text{ lbf}$
Bounding Weight of the Thoria Rod Canister (Estimated)	$W_{rodcan} := 300 \text{ lbf}$
Quality factor for full penetration weld (visual inspection)	$n := 0.5$
Dynamic load factor for lifting	$DLF := 1.15$

The remaining input data is provided as needed in the calculation section

### 3.AR.8 Calculations for Transnuclear Damaged Fuel Canister

#### 3.AR.8.1 Lifting Operation (Normal Condition)

The critical load case under normal conditions is the lifting operation. The key areas of concern for ASME NG analysis are the canister sleeve, the sleeve to lid frame weld, and the lid frame. All calculations performed for the lifting operation assume a dynamic load factor of 1.15 [1].

##### 3.AR.8.1.1 Canister Sleeve

During a lift, the canister sleeve is loaded axially, and the stress state is pure tensile membrane. For the subsequent stress calculation, it is assumed that the full weight of the damaged fuel canister and the fuel assembly are supported by the sleeve. The magnitude of the load is

$$F := DLF \cdot (W_{container} + W_{fuel}) \quad F = 632 \text{ lbf}$$

From TN drawing 9317.1-120-4, the canister sleeve geometry is

$$id_{sleeve} := 4.81 \text{ in} \quad t_{sleeve} := 0.11 \text{ in}$$

The cross sectional area of the sleeve is

$$A_{sleeve} := (id_{sleeve} + 2 \cdot t_{sleeve})^2 - id_{sleeve}^2 \quad A_{sleeve} = 2.16 \text{ in}^2$$

Therefore, the tensile stress in the sleeve is

$$\sigma := \frac{F}{A_{\text{sleeve}}} \quad \sigma = 292 \text{ psi}$$

The allowable stress intensity for the primary membrane category is  $S_m$  per Subsection NG of the ASME Code. The corresponding safety margin is

$$SM := \frac{S_{m1}}{\sigma} - 1 \quad SM = 67.5$$

### 3.AR.8.1.2 Sleeve Welds

The top of the canister must support the amplified weight. This load is carried directly by the fillet weld that connects the lid frame to the canister sleeve. The magnitude of the load is conservatively taken as the entire amplified weight of canister plus fuel.

$$F = 632 \text{ lbf}$$

The weld thickness is  $t_{\text{base}} := 0.09 \text{ in}$

The area of the weld, with proper consideration of quality factors, is

$$A_{\text{weld}} := n \cdot 4 \cdot (i_{\text{sleeve}} + 2 \cdot t_{\text{sleeve}}) \cdot 0.7071 \cdot t_{\text{base}} \quad A_{\text{weld}} = 0.64 \text{ in}^2$$

Therefore, the shear stress in the weld is

$$\tau := \frac{F}{A_{\text{weld}}} \quad \tau = 988 \text{ psi}$$

From the ASME Code the allowable weld shear stress, under normal conditions (Level A), is 30% of the ultimate strength of the base metal. The corresponding safety margin is

$$SM := \frac{0.3 S_{u1}}{\tau} - 1 \quad SM = 21.2$$

### 3.AR.8.1.3 Lid Frame Assembly

The Lid Frame assembly is classified as a NUREG-0612 lifting device. As such the allowable stress for design is the lesser of one-sixth of the yield stress and one-tenth of the ultimate strength.

$$\begin{aligned} \sigma_1 &= \frac{S_{y1}}{6} & \sigma_2 &:= \frac{S_{u1}}{10} \\ \sigma_1 &= 4583 \text{ psi} & \sigma_2 &= 7300 \text{ psi} \end{aligned}$$

For SA240-304 material the yield stress governs.  $\sigma_{\text{allowable}} := \sigma_1$

The total lifted load is  $F := \text{DLF} \cdot (W_{\text{container}} + W_{\text{fuel}})$   $F = 632 \text{ lbf}$

The frame thickness is obtained from Transnuclear drawing 9317.1-120-11

$$t_{\text{frame}} := 0.395 \text{ in}$$

The inside span is the same as the canister sleeve  $\text{id}_{\text{sleeve}} = 4.81 \text{ in}$

The area available for direct load is

$$A_{\text{frame}} := (\text{id}_{\text{sleeve}} + 2 \cdot t_{\text{frame}})^2 - \text{id}_{\text{sleeve}}^2 \quad A_{\text{frame}} = 8.224 \text{ in}^2$$

The direct stress in the frame is

$$\sigma := \frac{F}{A_{\text{frame}}} \quad \sigma = 77 \text{ psi}$$

The safety margin is

$$\text{SM} := \frac{\sigma_{\text{allowable}}}{\sigma} - 1 \quad \text{SM} = 58.59$$

The bearing stress at the four lift locations is computed from the same drawing

$$A_{\text{bearing}} := 4 \cdot t_{\text{frame}} \cdot (2 \cdot 0.38 \text{ in}) \quad A_{\text{bearing}} = 1.201 \text{ in}^2$$

$$\sigma_{\text{bearing}} := \frac{F}{A_{\text{bearing}}} \quad \sigma_{\text{bearing}} = 526.732 \text{ psi} \quad \text{SM} := \frac{\sigma_{\text{allowable}}}{\sigma_{\text{bearing}}} - 1 \quad \text{SM} = 7.7$$

3.AR.8.2 60g End Drop of HI-STAR 100 (Bounding Accident Condition since HI-STORM limit is 45g's)

The critical member of the damaged fuel canister during the drop scenario is the bottom assembly (see Transnuclear drawing 9317.1-120-5). It is subjected to direct compression due to the amplified weight of the fuel assembly and the canister. The bottom assembly is a 3.5" Schedule 40S pipe. The load due to the 60g end drop is

$$F := 60 \cdot (W_{\text{fuel}} + W_{\text{container}}) \quad F = 33000 \text{ lbf}$$

The properties of the pipe are obtained from the Ryerson Stock Catalog as

$$\text{od} := 4 \text{ in} \quad \text{id} := 3.548 \text{ in} \quad t_{\text{pipe}} := \frac{(\text{od} - \text{id})}{2} \quad t_{\text{pipe}} = 0.226 \text{ in}$$

The pipe area is

$$A_{\text{pipe}} := \frac{\pi}{4} \cdot (\text{od}^2 - \text{id}^2) \quad A_{\text{pipe}} = 2.68 \text{ in}^2$$

The stress in the member is

$$\sigma := \frac{F}{A_{\text{pipe}}} \quad \sigma = 12316 \text{ psi}$$

The allowable primary membrane stress from Subsection NG of the ASME Code, for accident conditions (Level D), is

$$\sigma_{\text{allowable}} := 2.4 \cdot S_{m2} \quad \sigma_{\text{allowable}} = 37920 \text{ psi}$$

The safety margin is

$$SM := \frac{\sigma_{\text{allowable}}}{\sigma} - 1 \quad SM = 2.1$$

To check the stability of the pipe, we conservatively compute the Euler Buckling load for a simply supported beam.

The Young's Modulus is

$$E := 27600000 \text{ psi}$$

Compute the moment of inertia as

$$I := \frac{\pi}{64} (\text{od}^4 - \text{id}^4) \quad I = 4.788 \text{ in}^4$$

$L := 22 \text{ m}$

$$P_{\text{crit}} := \pi^2 \frac{EI}{L^2} \quad P_{\text{crit}} = 2.695 \times 10^6 \text{ lbf}$$

The safety margin is

$$SM := \frac{P_{\text{crit}}}{F} - 1 \quad SM = 80.654$$

### 3.AR.8.3 Conclusion for TN Damaged Fuel Canister

The damaged fuel canister and the upper closure assembly are structurally adequate to withstand the specified normal and accident condition loads. All calculated safety margins are greater than zero.

### 3.AR.9 Calculations for Transnuclear Thoria Rod Canister

#### 3.AR.9.1 Lifting Operation (Normal Condition)

The critical load case under normal conditions is the lifting operation. The key areas of concern for ASME NG analysis are the canister sleeve, the sleeve to lid frame weld, and the lid frame. All calculations performed for the lifting operation assume a dynamic load factor of 1.15.

##### 3.AR.9.1.1 Canister Sleeve

During a lift, the canister sleeve is loaded axially, and the stress state is pure tensile membrane. For the subsequent stress calculation, it is assumed that the full weight of the Thoria rod canister and the Thoria rods are supported by the sleeve. The magnitude of the load is

$$F := DLF \cdot (W_{\text{rodcan}} + W_{\text{thoria}})$$

$$F = 449 \text{ lbf}$$

From TN drawing 9317.1-182-1, the canister sleeve geometry is

$$id_{\text{sleeve}} := 4.81 \text{ in}$$

$$t_{\text{sleeve}} := 0.11 \text{ in}$$

The cross sectional area of the sleeve is

$$A_{\text{sleeve}} := (id_{\text{sleeve}} + 2 \cdot t_{\text{sleeve}})^2 - id_{\text{sleeve}}^2$$

$$A_{\text{sleeve}} = 2.16 \text{ in}^2$$

Therefore, the tensile stress in the sleeve is

$$\sigma := \frac{F}{A_{\text{sleeve}}}$$

$$\sigma = 207 \text{ psi}$$

The allowable stress intensity for the primary membrane category is  $S_m$  per Subsection NG of the ASME Code. The corresponding safety margin is

$$SM := \frac{S_m}{\sigma} - 1$$

$$SM = 95.5$$

### 3.AR.9.1.2 Sleeve Welds

The top of the canister must support the amplified weight. This load is carried directly by the fillet weld that connects the lid frame to the canister sleeve. The magnitude of the load is conservatively taken as the entire amplified weight of canister plus Thoria rod.

$$F = 449 \text{ lbf}$$

The weld thickness is

$$t_{\text{base}} := 0.09 \text{ in}$$

(assumed equal to the same weld for the damaged fuel canister)

The area of the weld, with proper consideration of quality factors, is

$$A_{\text{weld}} := n \cdot 4 \cdot (id_{\text{sleeve}} + 2 \cdot t_{\text{sleeve}}) \cdot 0.7071 \cdot t_{\text{base}}$$

$$A_{\text{weld}} = 0.64 \text{ in}^2$$

Therefore, the shear stress in the weld is

$$\tau := \frac{F}{A_{\text{weld}}}$$

$$\tau = 701 \text{ psi}$$

From the ASME Code the allowable weld shear stress, under normal conditions (Level A), is 30% of the ultimate strength of the base metal. The corresponding safety margin is

$$SM := \frac{0.3 \cdot S_{ul}}{\tau} - 1$$

$$SM = 30.3$$

### 3.AR.9 1.3 Lid Frame Assembly

The Lid Frame assembly is classified as a NUREG-0612 lifting device. As such the allowable stress for design is the lesser of one-sixth of the yield stress and one-tenth of the ultimate strength.

$$\sigma_1 := \frac{S_{y1}}{6} \qquad \sigma_2 := \frac{S_{u1}}{10}$$

$$\sigma_1 = 4583 \text{ psi} \qquad \sigma_2 = 7300 \text{ psi}$$

For SA240-304 material the yield stress governs.  $\sigma_{\text{allowable}} := \sigma_1$

The total lifted load is  $F := \text{DLF} \cdot (W_{\text{rodcan}} + W_{\text{thoria}})$   $F = 449 \text{ lbf}$

The frame thickness is obtained from Transnuclear drawing 9317.1-182-8. This drawing was not available, but the TN drawing 9317.1-182-4 that included a view of the lid assembly suggests that it is identical in its structural aspects to the lid frame in the damaged fuel canister.

$$t_{\text{frame}} := 0.395 \text{ in}$$

The inside span is the same as the canister sleeve  $\text{id}_{\text{sleeve}} = 4.81 \text{ in}$

The area available for direct load is

$$A_{\text{frame}} := (\text{id}_{\text{sleeve}} + 2 t_{\text{frame}})^2 - \text{id}_{\text{sleeve}}^2 \qquad A_{\text{frame}} = 8.224 \text{ in}^2$$

The direct stress in the frame is

$$\sigma := \frac{F}{A_{\text{frame}}} \qquad \sigma = 55 \text{ psi}$$

The safety margin is

$$\text{SM} := \frac{\sigma_{\text{allowable}}}{\sigma} - 1 \qquad \text{SM} = 83.04$$

The bearing stress at the four lift locations is computed from the same drawing

$$A_{\text{bearing}} := 4 t_{\text{frame}} (2.038 \text{ in}) \qquad A_{\text{bearing}} = 1.201 \text{ in}^2$$

$$\sigma_{\text{bearing}} := \frac{F}{A_{\text{bearing}}} \qquad \sigma_{\text{bearing}} = 373.501 \text{ psi} \qquad \text{SM} := \frac{\sigma_{\text{allowable}}}{\sigma_{\text{bearing}}} - 1 \qquad \text{SM} = 11.27$$

### 3.AR.9.2 60g HI-STAR End Drop (Bounds Accident Condition in HI-STORM)

The critical member of the damaged fuel canister during the drop scenario is the bottom assembly. Transnuclear drawing 9317.1-120-5). It is subjected to direct compression due to the amplified weight of the Thoria rods and the canister.

$$F := 60 (W_{\text{thoria}} + W_{\text{rodcan}}) \quad F = 23400 \text{ lbf}$$

The properties of the pipe are obtained from the Ryerson Stock Catalog as

$$\text{od} := 4 \text{ in} \quad \text{id} := 3.548 \text{ in} \quad t_{\text{pipe}} := \frac{(\text{od} - \text{id})}{2} \quad t_{\text{pipe}} = 0.226 \text{ in}$$

The pipe area is

$$A_{\text{pipe}} := \frac{\pi}{4} (\text{od}^2 - \text{id}^2) \quad A_{\text{pipe}} = 2.68 \text{ in}^2$$

The stress in the member is

$$\sigma := \frac{F}{A_{\text{pipe}}} \quad \sigma = 8733 \text{ psi}$$

The allowable primary membrane stress from Subsection NG of the ASME Code, for accident conditions (Level D), is

$$\sigma_{\text{allowable}} := 2.4 \cdot S_{m2} \quad \sigma_{\text{allowable}} = 37920 \text{ psi}$$

The safety margin is

$$\text{SM} := \frac{\sigma_{\text{allowable}}}{\sigma} - 1 \quad \text{SM} = 3.3$$

To check the stability of the pipe, we compute the Euler Buckling load for a simply supported beam.

The Young's Modulus is

$$E := 27600000 \text{ psi}$$

Compute the moment of inertia as

$$I := \frac{\pi}{64} (\text{od}^4 - \text{id}^4) \quad I = 4.788 \text{ in}^4$$

$$L := 22 \text{ in}$$

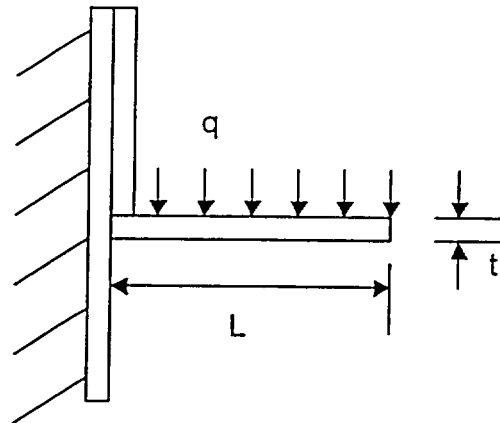
$$P_{\text{cnt}} := \pi^2 \cdot \frac{EI}{L^2} \quad P_{\text{cnt}} = 2.695 \times 10^6 \text{ lbf}$$

The safety margin is

$$\text{SM} := \frac{P_{\text{cnt}}}{F} - 1 \quad \text{SM} = 114.153$$

### 3.AR.9.4 60g HI-STAR Side Drop (Bounds Accident Condition for HI-STORM)

The Thoria Rod Separator Assembly is shown in TN drawings 9317.1-182-1 and 9317.1-182-3. under the design basis side drop or tipover accident, we examine the consequences to one of the rod support strips acting as a cantilever strip acted upon by self-weight and the weight of one Thoria rod.



Weight of 1 rod per unit length

$$\text{length} := 113.16 \cdot \text{in}$$

$$w_{\text{rod}} = 90 \frac{\text{lbf}}{18} \frac{1}{\text{length}}$$

$$w_{\text{rod}} = 0.044 \frac{\text{lbf}}{\text{in}}$$

Weight of support per unit length (per drawing 9317.1-182-3)

$$L := 1.06 \cdot \text{in}$$

$$t := 0.11 \cdot \text{in}$$

$$w_{\text{sup}} := 29 \frac{\text{lbf}}{\text{in}^3} \cdot L \cdot t$$

$$w_{\text{sup}} = 0.034 \frac{\text{lbf}}{\text{in}}$$

Amplified load (assumed as a uniform distribution)

$$q := 60 (w_{\text{rod}} + w_{\text{sup}})$$

$$q = 4.68 \frac{\text{lbf}}{\text{in}}$$

$$\text{Moment} := \frac{q \cdot L^2}{2}$$

$$\text{Moment} = 2.629 \text{ in} \cdot \text{lbf}$$

Bending stress at the root of the cantilever beam is

$$\sigma = 6 \cdot \frac{\text{Moment}}{1 \cdot \text{in} \cdot t^2}$$

$$\sigma = 1.304 \times 10^3 \text{ psi}$$

Shear stress at the root of the cantilever

$$\tau := q \frac{L}{t \cdot 1 \cdot \text{in}}$$

$$\tau = 45.098 \text{ psi}$$

Large margins of safety are indicated by these stress results.

### 3.AR.9.5 Conclusion for TN Thoria Rod Canister

The Thoria rod canister is structurally adequate to withstand the specified normal and accident condition loads. All calculated safety margins are greater than zero.

### 3.AR.10 General Conclusion

The analysis of the TN damaged fuel canister and the TN Thoria rod canister have demonstrated that all structural safety margins are large. We have confirmed that the TN canisters have positive safety margins for the HI-STAR 100 governing design basis loads. The HI-STAR design basis handling accident load bounds the corresponding load for HI-STORM. Therefore, the loaded TN canisters from ComEd Dresden Unit#1 can safely be carried in both the HI-STAR and HI-STORM 100 Systems.

### 3.AR.11 List of Transnuclear Drawing Numbers

9317.1-120 - 2,3,4,5,6,7,8,9,10,11,13,14,15,17,18,19,20,21,22,23

9317.1-182- 1,2,3,4,5,6

## APPENDIX 3.AS - ANALYSIS OF GENERIC PWR AND BWR DAMAGED FUEL CONTAINERS

### 3.AS.1 Introduction

This appendix contains an analysis of the damaged fuel containers that are used for the HI-STAR 100 MPC-24E and MPC-68, respectively. The objective of the analysis is to demonstrate that the two types of storage containers are structurally adequate to support the loads that develop during normal lifting operations and during an end drop.

The lifting bolt of each containers is designed to meet the requirements set forth for Special Lifting Devices in Nuclear Plants [2]. The remaining components of the damaged fuel container are compared to ASME Code Section III, Subsection NG allowable stress levels.

### 3.AS.2 Composition

This appendix was created using the Mathcad (version 2000) software package. Mathcad uses the symbol ':=' as an assignment operator, and the equals symbol '=' retrieves values for constants or variables.

### 3.AS.3 References

1. Crane Manufacture's of America Association, Specifications for Electric Overhead Traveling Cranes #70.
2. ANSI N14-6, Special Lifting Devices for Loads Greater than 10000 lbs. in Nuclear Plants.
3. ASME Boiler and Pressure Vessel Code, Section III Subsection NG, July 1995
4. Roark's Formulas for Stress & Strain, 6th Edition, 1989.
5. Kent's Mechanical Engineers' Handbook, Design and Production Volume, 12th Edition, 1965
6. ASME, "Boiler & Pressure Vessel Code," Section II, Part D-Material Properties, July 1, 1995

### 3.AS.4 Assumptions

1. Buckling is not a concern during an accident since during a drop the canister will be supported by the walls of the fuel basket.
2. The strength of the weld is assumed to decrease the same as the base metal as the temperature is increased.

### 3.AS.5 Method

Two cases are considered: 1) normal handling of container, and 2) accident drop event.

### 3.AS.6 Acceptance Criteria

#### 1) Normal Handling -

a) Container governed by ASME NG[3] allowables:  
shear stress allowable is 60% of membrane stress intensity

b) Welds are governed by NG Code allowables; stress limit = 60% of tensile stress intensity (per Section III, Subsection NG-3227.2).

c) Lifting bolt is governed by ANSI N14-6 criteria

#### 2) Drop Accident -

a) Container governed by ASME Section III, Appendix F allowables:  
(allowable shear stress = 0.42  $S_u$ )

### 3.AS.7 Input Data for MPC-24E (PWR) Damaged Fuel Container

The damaged fuel container is only handled while still in the spent fuel pool. Therefore, its design temperature for lifting considerations is the temperature of the fuel pool water (150°F). The design temperature for accident conditions is 725°F. All dimensions are taken from Dwg. 2776. The basic input parameters used to perform the calculations are:

Design stress intensity of SA240-304 (150°F)	$S_{m1} := 20000\text{-psi}$	Table 1.A.1
Design stress intensity of SA240-304 (725°F)	$S_{m2} := 15800\text{-psi}$	
Yield stress of SA240-304 (150°F)	$S_{y1} := 27500\text{-psi}$	Table 1.A.3
Yield stress of SA240-304 (725°F)	$S_{y2} := 17500\text{-psi}$	
Ultimate strength of SA240-304 (150°F)	$S_{u1} := 73000\text{-psi}$	Table 1.A.2
Ultimate strength of SA240-304 (725°F)	$S_{u2} := 63300\text{-psi}$	
Minimum Yield stress of SA564-630 (200°F)	$S_{by} := 97100\text{-psi}$	Table 2.3.5
Minimum Ultimate strength of SA564-630 (200°F)	$S_{bu} := 135000\text{-psi}$	

Weight of a PWR fuel assembly (allowable maximum value)	$W_{\text{fuel}} := 1507 \cdot \text{lbf}$
Weight of the damaged fuel container	$W_{\text{container}} := 173 \cdot \text{lbf}$
Wall thickness of the container sleeve	$t_{\text{sleeve}} := 0.075 \cdot \text{in}$
Dimension of the square baseplate	$d_{\text{bplate}} := 8.75 \cdot \text{in}$
Thickness of the baseplate	$t_{\text{bplate}} := 0.75 \cdot \text{in}$
Diameter of baseplate through hole	$d_{\text{bph}} := 2 \cdot \text{in}$
Number of baseplate through holes	$N_{\text{bph}} := 5$
Diameter of the baseplate spot weld	$d_{\text{wbase}} := 0.125 \cdot \text{in}$
Inner dimension of the container sleeve	$id_{\text{sleeve}} := 8.75 \cdot \text{in}$
Wall thickness of container collar	$t_{\text{collar}} := 0.21 \cdot \text{in}$
Distance from end of sleeve to top of engagement slot	$d_{\text{slot}} := 0.1875 \cdot \text{in}$
Thickness of the load tab	$t_{\text{tab}} := 0.125 \cdot \text{in}$
Width of the load tab	$w_{\text{tab}} := 2.0 \cdot \text{in}$
Thickness of the closure plate	$t_{\text{cp}} := 0.5 \cdot \text{in}$
Radius of the lifting bolt	$r_{\text{bolt}} := 0.1875 \cdot \text{in}$
Weight density of the stainless steel	$\gamma_{\text{ss}} := 0.283 \cdot \frac{\text{lbf}}{\text{in}^3}$
Thickness of the nut	$t_{\text{nut}} := 0.346 \cdot \text{in} \quad [5]$
Length of the bolt	$L_{\text{bolt}} := 2.0 \cdot \text{in}$
Height of the bolt head	$t_{\text{bolt}} := 0.268 \cdot \text{in} \quad [5]$
Thickness of the washer	$t_{\text{washer}} := 0.125 \cdot \text{in}$
Dynamic load factor for lifting [1]	$\text{DLF} := 1.15$

### 3.AS.7 Calculations for MPC-24E Damaged Fuel Container

#### 3.AS.7.1 Lifting Operation (Normal Condition)

The critical load case under normal conditions is the lifting operation. The key areas of concern are the container sleeve, the weld between the sleeve and the base of the container, the container upper closure, and the lifting bolt. All calculations performed for the lifting operation assume a dynamic load factor of 1.15.

##### 3.AS.7.1.1 Container Sleeve (Item 1)

During a lift, the container sleeve is loaded axially, and the stress state is pure tensile membrane. For the subsequent stress calculation, it is assumed that the full weight of the damaged fuel container and the fuel assembly are supported by the sleeve. The magnitude of the load is

$$F := \text{DLF} \cdot (W_{\text{container}} + W_{\text{fuel}}) \quad F = 1932 \text{ lbf}$$

The cross sectional area of the sleeve is

$$A_{\text{sleeve}} := (i_{\text{sleeve}} + 2 \cdot t_{\text{sleeve}})^2 - i_{\text{sleeve}}^2 \quad A_{\text{sleeve}} = 2.65 \text{ in}^2$$

Therefore, the tensile stress in the sleeve is

$$\sigma := \frac{F}{A_{\text{sleeve}}} \quad \sigma = 730 \text{ psi}$$

The allowable stress intensity for the primary membrane category is  $S_m$  per Subsection NG of the ASME Code. The corresponding safety factor is

$$\text{SF} := \frac{S_m}{\sigma} \quad \text{SF} = 27.4$$

##### 3.AS.7.1.2 Base Weld (Between Item 1 and Item 7)

The base of the container must support the amplified weight of the fuel assembly. This load is carried directly by 16 spot welds (4 on each side) which connect the base to the container sleeve. The weight of the baseplate is

$$W_{\text{bplate}} := \left( d_{\text{bplate}}^2 - N_{\text{bph}} \cdot \frac{\pi}{4} \cdot d_{\text{bph}}^2 \right) \cdot t_{\text{bplate}} \cdot \gamma_{\text{ss}} \quad W_{\text{bplate}} = 13 \text{ lbf}$$

The total load carried by the spot welds is

$$F := \text{DLF} \cdot (W_{\text{fuel}} + W_{\text{bplate}}) \quad F = 1748 \text{ lbf}$$

The area of the weld is

$$A_{\text{weld}} := 4.4 \frac{3.14 \cdot d \cdot w_{\text{base}}^2}{4} \quad A_{\text{weld}} = 0.2 \text{ in}^2$$

Therefore, the amplified shear stress in the weld is

$$\sigma := \frac{F}{A_{\text{weld}}} \quad \sigma = 8907 \text{ psi}$$

From the ASME Code the allowable weld shear stress, under normal conditions (Level A), is 60% of the membrane strength of the base metal. The corresponding safety factor is

$$\text{SF} := \frac{0.6 \cdot S_{m1}}{\sigma} \quad \text{SF} = 1.3$$

### 3.AS.7.1.3 Container Collar (Items 1 and 2)

The load tabs of the upper lock device engage the container collar during a lift. The load transferred to the engagement slot, by a single tab, is

$$F := \frac{\text{DLF} \cdot (W_{\text{container}} + W_{\text{fuel}})}{4} \quad F = 483 \text{ lbf}$$

The shear area of the container collar is

$$A_{\text{collar}} := 2 \cdot d_{\text{slot}} \cdot (t_{\text{sleeve}} + t_{\text{collar}}) \quad A_{\text{collar}} = 0.107 \text{ in}^2$$

The shear stress in the collar is

$$\sigma := \frac{F}{A_{\text{collar}}} \quad \sigma = 4519 \text{ psi}$$

The allowable shear stress from Subsection NG, under normal conditions, is

$$\sigma_{\text{allowable}} := 0.6 S_{m1} \quad \sigma_{\text{allowable}} = 12000 \text{ psi}$$

Therefore, the safety factor is

$$SF := \frac{\sigma_{\text{allowable}}}{\sigma} \quad SF = 2.7$$

### 3.AS.7.1.4 Load Tabs (Item 3)

The load tabs of the lock device engage the container collar during a lift. The shear area of each tab is

$$A_{\text{tab}} := t_{\text{tab}} \cdot w_{\text{tab}} \quad A_{\text{tab}} = 0.25 \text{ in}^2$$

The shear stress in the tab is

$$\tau_{\text{tab}} := \frac{F}{A_{\text{tab}}} \quad \tau_{\text{tab}} = 1.932 \times 10^3 \text{ psi}$$

Therefore, the safety factor is

$$SF := \frac{0.6 \cdot S_{m1}}{\tau_{\text{tab}}} \quad SF = 6.211$$

### 3.AS.7.1.4 Upper Closure (Item 4)

The damaged fuel container is lifted by a bolt at the center of the upper closure plate. Assuming that the square upper closure plate is simply supported at the boundary and loaded by a uniform concentric circle of radius of the bolt, we can use the formula given in Table 26 of Ref. [4] to calculate the maximum bending stress of the plate. For a square plate, the coefficient of the stress formula is:

$$\beta := 0.435$$

The maximum bending stress in the plate is

$$\sigma_{\text{max}_c} := \frac{3 \cdot (W_{\text{container}} + W_{\text{fuel}}) \cdot \text{DLF}}{2 \cdot \pi \cdot t_{\text{cp}}^2} \cdot \left[ (1 + 0.3) \cdot \ln \left( \frac{2 \cdot \text{id}_{\text{sleeve}}}{\pi \cdot r_{\text{bolt}}} \right) + \beta \right]$$

$$\sigma_{\text{max}_c} = 1.787 \times 10^4 \text{ psi}$$

The allowable primary stress for the plate, per Subsection NG of ASME code, is

$$\sigma_{\text{allowable\_cp}} := 1.5 S_{m1}$$

$$\sigma_{\text{allowable\_cp}} = 3 \times 10^4 \text{ psi}$$

Safety factor

$$SF := \frac{\sigma_{\text{allowable\_cp}}}{\sigma_{\text{max\_c}}}$$

$$SF = 1.678$$

### 3.AS.7.1.5 Lifting Bolt (Item 5)

The stress area of the 1/2-12UNC bolt is

$$A_{\text{bolt}} := 0.0773 \text{ in}^2 \quad [5]$$

The tensile stress in the bolt

$$\sigma_{\text{bolt}} := \frac{(W_{\text{container}} + W_{\text{fuel}}) \cdot \text{DLF}}{A_{\text{bolt}}}$$

$$\sigma_{\text{bolt}} = 2.499 \times 10^4 \text{ psi}$$

The lifting bolt must meet the requirements set forth for Special Devices [2]. As such the allowable tensile stress for design is the lesser of one-third of the yield stress and one-fifth of the ultimate strength.

$$\sigma_1 := \frac{S_{by}}{3}$$

$$\sigma_2 := \frac{S_{bu}}{5}$$

$$\sigma_1 = 32367 \text{ psi}$$

$$\sigma_2 = 27000 \text{ psi}$$

For SA193-B8 material the yield stress governs at the lifting temperature.

$$\sigma_{\text{allowable}} := \sigma_2$$

Safety factor

$$SF := \frac{\sigma_{\text{allowable}}}{\sigma_{\text{bolt}}}$$

$$SF = 1.08$$

Now check the thread engagement of the bolt. The minimum required length of the bolt is

$$L_{\text{engage}} := t_{\text{cp}} + t_{\text{washer}} + t_{\text{tab}} + 2 \cdot t_{\text{nut}}$$

$$L_{\text{engage}} = 1.442 \text{ in}$$

The length of the bolt is

$$L_{\text{bolt}} = 2 \text{ in}$$

Therefore, the thread engagement requirement is satisfied.

### 3.AS.7.2 60g End Drop (Accident Condition)

The critical member of the damaged fuel container, during a postulated upside down end drop scenario, is the 16 spot welds. The total load applied to the welds in a 60g end drop is

$$F_{\text{drop}} := 60 \cdot W_{\text{bplate}} \quad F_{\text{drop}} = 774.983 \text{ lbf}$$

$$\sigma := \frac{F_{\text{drop}}}{A_{\text{weld}}} \quad \sigma = 3949 \text{ psi}$$

$$\sigma_{\text{allowable}} := 0.42 \cdot S_{u2} \quad \sigma_{\text{allowable}} = 26586 \text{ psi}$$

The safety factor is

$$SF := \frac{\sigma_{\text{allowable}}}{\sigma}$$

$$SF = 6.7$$

### 3.AS.8 Input Data for MPC-68 BWR Damaged Fuel Container

The damaged fuel container is only handled while still in the spent fuel pool. Therefore, its design temperature for lifting considerations is the temperature of the fuel pool water (150°F). The design temperature for accident conditions is 725°F. All dimensions are taken from the Dwg. 2775. The basic input parameters used to perform the calculations are:

Design stress intensity of SA240-304 (150°F)	$S_{m1} := 20000 \text{ psi}$	Table 1.A.1
Design stress intensity of SA240-304 (725°F)	$S_{m2} := 15800 \text{ psi}$	
Yield stress of SA240-304 (150°F)	$S_{y1} := 27500 \text{ psi}$	Table 1.A.3
Yield stress of SA240-304 (725°F)	$S_{y2} := 17500 \text{ psi}$	
Ultimate strength of SA240-304 (150°F)	$S_{u1} := 73000 \text{ psi}$	Table 1.A.2
Ultimate strength of SA240-304 (725°F)	$S_{u2} := 63300 \text{ psi}$	
Total weight of the loaded container	$W_{\text{load}} := 700 \text{ lbf}$	
Wall thickness of the container sleeve	$t_{\text{sleeve}} := 0.035 \text{ in}$	

Dimension of the square baseplate	$d_{\text{bplate}} := 5.7 \cdot \text{in}$
Thickness of the baseplate	$t_{\text{bplate}} := 0.5 \cdot \text{in}$
Diameter of baseplate through hole	$d_{\text{bph}} := 1.25 \cdot \text{in}$
Number of baseplate through holes	$N_{\text{bph}} := 4$
Diameter of spot welds	$d_{\text{wbase}} := 0.125 \cdot \text{in}$
Inner dimension of the container sleeve	$i_{\text{dsleeve}} := 5.701 \cdot \text{in}$
Thickness of the tube cap top plate	$t_{\text{cap_tp}} := 0.5 \cdot \text{in}$
Diameter of the hole on the top plate	$d_{\text{tph}} := 1.25 \cdot \text{in}$
Thickness of the tube cap side plate	$t_{\text{cap_sp}} := 0.035 \cdot \text{in}$
Width of the side plate	$w_{\text{sp}} := 4 \cdot \text{in}$
Length of the locking slot	$L_{\text{slot}} := 3.05 \cdot \text{in}$
Width of locking slot	$w_{\text{slot}} := 0.34 \cdot \text{in}$
Distance between locking bar center to the top plate bottom	$L_{\text{bar}} := 1.5 \cdot \text{in}$
Thickness of locking bar	$t_{\text{bar}} := 0.1 \cdot \text{in}$
Width of the locking bar	$w_{\text{l_bar}} := 0.25 \cdot \text{in}$
Diameter of the lifting bolt	$d_{\text{bolt}} := 1.0 \cdot \text{in}$
Length of the lifting bolt	$L_{\text{bolt}} := 1.0 \cdot \text{in}$
Stress area of the bolt	$A_{\text{bolt}} := 0.6051 \cdot \text{in}^2$
Weld size at the bolt and top plate connection	$ww_{\text{bolt}} := \frac{1}{16} \cdot \text{in}$
Weight density of the stainless steel	$\gamma_{\text{ss}} := 0.283 \cdot \frac{\text{lbf}}{\text{in}^3}$
Dynamic load factor for lifting [1]	$\text{DLF} := 1.15$

### 3.AS.9 Calculations for MPC-68 Damaged Fuel Container

#### 3.AS.9.1 Lifting Operation (Normal Condition)

The critical load case under normal conditions is the lifting operation. The key areas of concern are the container sleeve, the spot welds, the tube cap plates, and the lifting bolt. All calculations performed for the lifting operation assume a dynamic load factor of 1.15.

##### 3.AS.9.1.1 Container Sleeve (Item 1)

During a lift, the container sleeve is loaded axially, and the stress state is pure tensile membrane. For the subsequent stress calculation, it is assumed that the full weight of the damaged fuel container and the fuel assembly are supported by the sleeve. The magnitude of the load is

$$F := DLF \cdot W_{\text{load}} \qquad F = 805 \text{ lbf}$$

The minimum cross sectional area, located at the locking slot elevation, of the sleeve is

$$A_{\text{sleeve}} := (id_{\text{sleeve}} + 2 \cdot t_{\text{sleeve}})^2 - id_{\text{sleeve}}^2 - 4 \cdot L_{\text{slot}} \cdot t_{\text{sleeve}} \qquad A_{\text{sleeve}} = 0.38 \text{ in}^2$$

Therefore, the tensile stress in the sleeve is

$$\sigma := \frac{F}{A_{\text{sleeve}}} \qquad \sigma = 2 \times 10^3 \text{ psi}$$

The allowable stress intensity for the primary membrane category is  $S_m$  per Subsection NG of the ASME Code. The corresponding safety factor is

$$SF := \frac{S_m}{\sigma} \qquad SF = 9.3$$

The tube may tearout at those four slots. From the ASME Code the allowable shear stress, under normal conditions (Level A), is 60% of the membrane strength of the metal. The minimum distance between the slot center line to top edge of the tube is determined as

$$d_{\text{slot}} := \frac{F}{0.6 \cdot S_m \cdot 8 \cdot t_{\text{sleeve}}} + \frac{w_{\text{slot}}}{2} \qquad d_{\text{slot}} = 0.41 \text{ in}$$

The tube won't tearout since the center line of the slot is located below the top edge at a distance of

$$L_{\text{bar}} = 1.5 \text{ in}$$

### 3.AS.9.1.2 Spot Weld

Some of the container parts are connected by spot welds at three locations: (1) between base plate of the container and the sleeve (2) between the locking bars and the tube cap side plates, and (3) between the tube cap side plates and the top plate. At each location, there are at least 12 spot welds to carry the load. To evaluate the structural integrity of these spot welds, the load applied to the welds is conservatively assumed to be the weight of the fully loaded container in each case.

The total load carried by the spot welds is

$$F := DLF \cdot W_{load} \qquad F = 8051 \text{bf}$$

The minimum total area of the weld connection is

$$A_{weld} := 12 \cdot \frac{3.14 \cdot d_{w_{base}}^2}{4} \qquad A_{weld} = 0.15 \text{in}^2$$

Therefore, the amplified shear stress in the weld is

$$\sigma := \frac{F}{A_{weld}} \qquad \sigma = 5469 \text{psi}$$

From the ASME Code the allowable weld shear stress, under normal conditions (Level A), is 60% of the membrane strength of the base metal. The corresponding safety factor is

$$SF := \frac{0.6 \cdot S_{m1}}{\sigma} \qquad SF = 2.2$$

### 3.AS.9.1.3 Tube cap top plate (Item 2A)

The damaged fuel container is lifted through a lifting bolt welded to the center of the tube cap top plate. Assuming that the square top plate is simply supported at the boundary and loaded by a uniform concentric circle of radius of the bolt, we can use the formula given in Table 26 of Ref. [4] to calculate the maximum bending stress in the plate. For a square plate, the coefficient in the stress formula is:

$$\beta := 0.435 \qquad r_{bolt} := \frac{d_{bolt}}{2}$$

The maximum bending stress in the plate is

$$\sigma_{max\_c} := \frac{3 \cdot W_{load} \cdot DLF}{2 \cdot \pi \cdot t_{cap\_tp}^2} \left[ (1 + 0.3) \cdot \ln \left( \frac{2 \cdot id_{sleeve}}{\pi \cdot r_{bolt}} \right) + \beta \right]$$

$$\sigma_{\max_c} = 4\,631 \times 10^3 \text{ psi}$$

Safety factor  $SF := \frac{\sigma_{\text{allowable\_cp}}}{\sigma_{\max_c}} \quad SF = 6.479$

### 3.AS.9.1.4 Tube cap side plate (Item 2B)

Four locking bars are welded to each of the four side plates. These side plates are bent to allow the locking bars to fit into the slots of the tube for lifting the container. Subsequent to bending, the side plates are forced to be vertical by the locking "ring" which pushes the locking bars into the slots in the container walls. While the side plates are deformed into the plastic range during the initial insertion over the canister tube process, the lowering of the locking ring reverses the state of stress in the side plates. It is required that the side plate should not reach the ultimate stress value during this single cycle of loading .

Deflection of the side plate  $d_{sp} := t_{\text{bar}} \quad d_{sp} = 0.1 \text{ in}$

The bending stress of the side plate is calculated by assuming that the side plate behaves as a cantilever beam.

$$E_{sp} := 2.7 \cdot 10^7 \cdot \text{psi} \quad L_{\text{bend\_sp}} := L_{\text{bar}} + \frac{W_{\text{bar}}}{2}$$

$$\sigma_{sp} := \frac{1.5 E_{sp} \cdot d_{sp} \cdot t_{\text{cap\_sp}}}{L_{\text{bend\_sp}}^2} \quad \sigma_{sp} = 5\,368 \times 10^4 \text{ psi}$$

The bending stress is less than the ultimate stress of the material (73 ksi) and therefore acceptable.

### 3.AS.9.1.5 Lifting Bolt (Item 5)

The stress area of the bolt is  $A_{\text{bolt}} = 0.605 \text{ in}^2$

The tensile stress in the bolt  $\sigma_{t\_bolt} := \frac{W_{\text{load}} \cdot DLF}{A_{\text{bolt}}} \quad \sigma_{t\_bolt} = 1.33 \times 10^3 \text{ psi}$

The lifting bolt must meet the requirements set forth for Special Devices [2]. As such the allowable tensile stress for design is the lesser of one-third of the yield stress and one-fifth of the ultimate strength.

$$\sigma_1 := \frac{S_{y1}}{3} \quad \sigma_1 = 9167 \text{ psi} \quad \sigma_2 := \frac{S_{u1}}{5} \quad \sigma_2 = 14600 \text{ psi}$$

For SA240-304 material the yield stress governs at the lifting temperature.

$$\sigma_{\text{allowable}} := \sigma_1$$

Safety factor  $SF := \frac{\sigma_{\text{allowable}}}{\sigma_{t\_bolt}} \quad SF = 6.89$

The bolt is welded to the tube cap top plate by the 1/16 fillet weld surrounding the periphery of the bolt. The shear stress in the weld is

$$\tau_{b\_weld} := \frac{DLF \cdot W_{\text{load}}}{\pi \cdot d_{\text{bolt}} \cdot (0.707 \cdot w_{w_{\text{bolt}}})} \quad \tau_{b\_weld} = 5.799 \times 10^3 \text{ psi}$$

From the ASME code the allowable weld shear stress, under normal condition (level A), is 60% of the membrane strength of the base metal. The corresponding safety factor is

$$SF := \frac{0.6 S_{m1}}{\tau_{b\_weld}} \quad SF = 2.069$$

### 3.AS.9.2 60g End Drop (Accident Condition)

The critical member of the damaged fuel container, under a postulated top down end drop scenario (that would occur only when the MPC is in transit), is the 16 spot welds. The total load applied to the welds in a 60g end drop (while installed in a HI-STAR 100 overpack) is

$$W_{\text{bplate}} := \left( d_{\text{bplate}}^2 - N_{\text{bph}} \cdot \frac{\pi}{4} \cdot d_{\text{bph}}^2 \right) \cdot t_{\text{bplate}} \cdot \gamma_{ss} \quad W_{\text{bplate}} = 4 \text{ lbf}$$

$$F_{\text{drop}} := 60 W_{\text{bplate}} \quad F_{\text{drop}} = 234.165 \text{ lbf}$$

$$\sigma := \frac{F_{\text{drop}}}{A_{\text{weld}}} \quad \sigma = 1591 \text{ psi} \quad \sigma_{\text{allowable}} := 0.42 \cdot S_{u2} \quad \sigma_{\text{allowable}} = 26586 \text{ psi}$$

The safety factor is

$$SF := \frac{\sigma_{\text{allowable}}}{\sigma} \quad SF = 16.7$$

### 3.AS.10 Conclusion

Both of the two types of damaged fuel containers are structurally adequate to withstand the specified normal and accident condition loads. All calculated safety factors are greater than one, which demonstrates that all acceptance criteria have been met or exceeded.